difficulty as only one of the two possible Z^*_α values is reasonable.

[22]J. C. Slater, Phys. Rev. **36**, 57 (1930).

[23]This similarity is important, since varying the type of anion (e.g., MnS) or crystal structure (e.g., TiO_2) will complicate the simple regularities exhibited in Table III.

[24]C. R. Jeggo and G. D. Boyd, J. Appl. Phys. **41**, 2741 (1970).

[25]J. L. Shay, B. Tell, H. M. Kasper, and L. M. Schiavone, Phys. Rev. B **5**, 5003 (1972).

[26]G. D. Boyd, H. Kasper, and J. H. McFee, IEEE J. Quantum Electron. **7**, 563 (1971).

PHYSICAL REVIEW B VOLUME 7, NUMBER 6 15 MARCH 1973

Bond-Charge Calculation of Nonlinear Optical Susceptibilities for Various Crystal Structures

B. F. Levine
Bell Laboratories, Murray Hill, New Jersey 07974
(Received 17 August 1972)

A simple localized-bond-charge model for the calculation of nonlinear optical susceptibilities is presented. We find that there are three important contributions to the nonlinearity, namely, the bond ionicity, the difference in atomic radii of the bonded atoms, and d-electron contributions. By including these effects we are able with one simple theory to accurately treat a wide variety of different types of compounds including $A^{III}B^{V}$ (e.g., GaAs, GaP, InSb), $A^{II}B^{VI}$ (e.g., ZnS, ZnO, BeO), $A^{I}B^{VII}$ (e.g., CuCl, CuBr, CuI), $A^{IV}B_2^{VI}$ (e.g., SiO_2), multibond crystals [e.g., $A^{I}B^{III}C_2^{VI}$ ($LiGaO_2$, $AgGaS_2$, $CuInS_2$, $CuGaSe_2$), $A^{II}B^{IV}C_2^{V}$ ($CdGeP_2$, $CdGeAs_2$, $ZnGeP_2$), $A^{III}B^{V}C_4^{VI}$ ($AlPO_4$), also KH_2PO_4], highly anisotropic crystals (e.g., HgS, Se, Te), as well as ferroelectrics (e.g., $LiNbO_3$, $Ba_2NaNb_5O_{15}$, $LiTaO_3$).

I. INTRODUCTION

There has been a substantial effort[1-35] devoted to understanding the origin of the linear[1,2] χ_{ij} and nonlinear optical susceptibility d_{ijk}, defined as

$$P_i(t) = \chi_{ij} E_j(t) + 2d_{ijk} E_j(t) E_k(t) , \qquad (1)$$

where P is the time-dependent polarization produced by an oscillating electric field $E(t) = E\cos\omega t$. Part of this interest in d_{ijk} has been motivated by the large nonlinearities observable with high-power lasers, which lead to such practical devices as efficient harmonic generators, optical mixers, and tunable parametric oscillators.[36] This nonlinearity d_{ijk} is also of great fundamental interest since it is sensitive to the asymmetric part of the charge distribution. That is, d_{ijk} vanishes for a free isolated atom, and hence its magnitude and sign in a crystal are strongly related to atomic interactions in solids, e.g., chemical bonding.

There have been many types of theoretical calculations of the nonlinear optical susceptibility. One approach starts with a perturbation expansion which expresses d_{ijk} in terms of complex sums of matrix elements and energy denominators.[3-10] This first-principles method is appealing since if one knew the complete band structure of the solid, one could directly evaluate d_{ijk} using no adjustable parameters. It is important to note that, since the many terms in the perturbation expressions tend to cancel one another, highly accurate wave functions are necessary (except in the x-ray region where an exact evaluation of the dominant term is possible).[11]

An important advance in greatly simplifying these complex-matrix-element sums was made by Robinson,[12] who related the nonlinear susceptibility to the octupole moment of the ground-state charge distribution. A similar approach using tetrahedral bonding orbitals for the ground-state wave function was later used by Jha and Bloembergen.[13] Flytzanis and Ducuing[14] did a more accurate calculation along these lines, using molecular orbitals determined from a four-parameter variational procedure. Another approach to the problem of simplifying the complex expressions for the nonlinear susceptibility is the constant-matrix-element approximation.[15-17] As shown by Aspnes[16] and Bell[17] contributions to the nonlinearity from a number of different points in the Brillouin zone must be included, with the result depending strongly on the various energy gaps involved. Coulomb interactions (related to local-field effects) have also been shown to be important.[16]

Other simple models for acentric solids include Miller's rule,[18] the free-electron model,[19] the anharmonic-oscillator model,[20-24] experimentally determined bond nonlinearities,[25-27] electric-field-induced energy-band shifts in ferroelectrics,[28] a charge-transfer model,[29] a relationship between the nonlinearity and the polarization in polar materials,[30] a two-band model using the Phillips and Van Vechten dielectric theory,[31,32] and the bond-charge model.[33-35]

This paper discusses the latter approach, which gives better experimental agreement than previous

calculations; but what is perhaps even more important is its capacity to deal with a wide range of complex crystal structures, many of which have never been treated before.

The organization of this paper is as follows: Section II treats the important bond-charge concept in detail and makes contact with the linear χ of Phillips[37] and Van Vechten.[38] Since the nonlinear optical susceptibility d_{ijk} is more highly sensitive to the crystal potentials than is the linear χ, it is necessary to generalize the work of Phillips and Van Vechten to obtain more accurate potentials; this is done in Sec. III.

These developments provide the basis for the derivation of the magnitude and sign of d_{ijk} and Δ_{ijk} in Secs. IV and V. The tetrahedral AB semiconductors such as GaAs are discussed in Sec. VI A; those containing first-row atoms or noble metals are treated in Secs. VI B and VI C. After reviewing the results on these compounds in Sec. VII, we turn to more complex crystals such as SiO_2 (Sec. VIII); $NaClO_3$ and $NaBrO_3$ (Sec. IX); $A^{I}B^{III}C_2^{VI}$ multibond compounds such as $LiGaO_2$ (Sec. X); $A^{II}B^{IV}C_2^{V}$, e.g., $CdGeAs_2$ (Sec. XI); $A^{III}B^{V}C_4^{VI}$, e.g., $AlPO_4$ (Sec. XII); $A^{I}B^{III}C_2^{VI}$, e.g., $AgGaS_2$ (Sec. XIII); KH_2PO_4 (Sec. XIV); ferroelectrics, e.g., $LiNbO_3$, $Ba_2NaNb_5O_{15}$ (Sec. XV); and highly anisotropic bonds, e.g., HgS, Se, Te (Sec. XVI). We comment on the favorable bond properties which lead to large nonlinearities in Sec. XVII and summarize our results in Sec. XVIII.

II. BOND CHARGE

It has been rather well established, both theoretically[39] and experimentally,[40] that the formation of a covalent bond produces an excess of charge in the bonding region. This bond formation greatly increases the crystal susceptibility, because the gradient of the crystal potential in the bonding region is lower than in the nonbonding directions. The bond charge q is thus weakly bound and highly mobile, whereas the spherical screening charge around the atom is tightly bound and makes only a small contribution to the susceptibility. We will assume that it is the dynamics of this bond charge q that are responsible for virtually all the measured susceptibility, that is, not only the linear susceptibility χ_{ij} but the nonlinear susceptibility d_{ijk} as well.

The bond charge may be thought of as arising from two sources. One is the contribution from the overlap of the spherical part of the atomic form factors q_0; the other contribution arises from the incomplete screening of the ion cores q_s. The total bond charge q that is moved by an applied electric field $\mathcal{E}$ is thus given by

$$q = q_s + q_o . \tag{2}$$

To evaluate q_s we will use the argument given by Phillips.[41] Consider first an AB semiconductor having Z_A and Z_B valence electrons on atoms A and B, respectively. The bare core of A thus has a positive charge $+Z_A(-e)$, where e is the electronic charge ($e<0$). The valence electrons surrounding atom A will, however, screen this bare charge and reduce it to $+Z_A(-e)/\epsilon$, where ϵ is the low-frequency electronic dielectric constant. The total remaining charge on the AB pair is thus $+(Z_A+Z_B)(-e)/\epsilon = +8(-e)/\epsilon$. Since there must be over-all charge neutrality there is a total charge $8e/\epsilon$ residing in the four bonds, i.e., $2e/\epsilon$ per bond. Martin[39] gets good results for the elastic constants using this value of $2e/\epsilon$. More generally $q = n_v e/\epsilon$, where n_v is the number of electrons per formula unit divided by the number of bonds per formula unit. For example $n_v = \frac{8}{4} = 2$ for AB semiconductors, while $n_v = \frac{16}{4} = 4$ for quartz (SiO_2).

The remaining contribution q_o is related to the rate of falloff of the atomic wave functions. For a highly ionic crystal (small f_c) the electrons are tightly bound and hence the overlap is small; conversely, for highly covalent bonds (large f_c) the electrons are delocalized implying a large overlap and a large q_o. We represent this close dependence between q_o and f_c by $q_o \propto f_c$. Hence

$$q/e = n_v(1/\epsilon + k f_c) . \tag{3}$$

One way of estimating the unknown constant k is to assume that q obeys simple trends and that, for example, the charge for Ge (which lies between Si and Sn in the fourth column of the Periodic Table) is the average of that for Si and Sn. That is

$$q(\mathrm{Ge}) = \tfrac{1}{2}[q(\mathrm{Si}) + q(\mathrm{Sn})] . \tag{4}$$

If we use the values $f_c = 1$ and $\epsilon = 12$, 16, and 24 for Si, Ge, and Sn, respectively,[38] in Eqs. (3) and (4), we obtain

$$(\tfrac{1}{16} + k) = \tfrac{1}{2}(\tfrac{1}{12} + k + \tfrac{1}{24} + k) = (\tfrac{1}{16} + k) , \tag{5}$$

which is an identity, independent of the value of k. Although this is therefore useless for determining k, it provides additional evidence for the validity of Eq. (3). Trends for any other similar set of compounds (e.g., GaAs, InAs, GaSb, InSb) are also insensitive to the precise value for k.

Fortunately there is a more accurate and direct method for determining k. Since we want to use our model to calculate the second-order (i.e., nonlinear) susceptibility, it is appropriate to ensure that this model is consistent with the lower-order linear susceptibility χ. We should therefore determine the unknown parameters (e.g., ionicity f_i, ionic gap C, charge-overlap constant k, etc.) using χ. In order to do this we use the bond-charge equation of motion

$$\frac{d^2}{dt^2}(\Delta r) + E_g^2(\Delta r) = \frac{q\mathcal{E}_L}{m} , \tag{6}$$

where Δr is the displacement from equilibrium, E_g is the Phillips[37] and Van Vechten[38] average energy gap, m is the electron mass, and $\mathcal{E}_L$ is the local electric field at the site of the bond charge. That is $\mathcal{E}_L = f\mathcal{E}$, where $\mathcal{E}$ is the applied electric field and f is the local-field factor. The polarization P produced by this displacement is

$$P = \chi\mathcal{E} = N_b q\,\Delta r\,, \tag{7}$$

where χ is the macroscopic susceptibility and N_b the number of bond charges per cm^3. Equations (6) and (7) yield the low-frequency electronic susceptibility

$$\chi = \frac{1}{4\pi}\,\frac{(\hbar\omega_q)^2}{E_g^2}\,f\,, \tag{8a}$$

where

$$\omega_q^2 = 4\pi N_b q^2/m \tag{8b}$$

and ω_q is the bond-charge plasma frequency.

In our model we neglect any bond-bond interactions; and so far as the localized isolated bonds are concerned the local-field factor required is just the full Lorentz expression $f_L = \frac{1}{3}(\epsilon + 2)$ (for cubic symmetry). Other authors[42] who use a more delocalized picture of these semiconductors need to use a smaller f.

All the quantities in Eqs. (8) are known with the exception of q; thus, using the experimental χ, E_g, etc., we can determine a value for the bond charge $q(\chi)$, which is listed in the first column of Table I for all the 20 IV-IV and III-V semiconductors. These crystals have been used since they are largely covalent, so that the simple harmonic oscillator Eq. (6) should be an adequate description. For crystals as ionic as the II-VI's or I-VII's the potential in the bonding region is so strong and asymmetric that Eq. (6) may be inadequate.

We can now determine the best value for k by obtaining the best one-parameter fit of Eq. (3) to $q(\chi)$; i.e., we set the average value of $q(\chi)$ equal to the average of the q calculated from Eq. (3), q(calc). This yields $k = 0.33$. The second column of Table II gives the results of calculating the bond charge from Eq. (3) with $k = 0.33$. We can compare the agreement between $q(\chi)$ and q(calc) by evaluating the quantity

$$\left[\frac{1}{n}\sum_1^n\left(\frac{q(\chi) - q(\text{calc})}{q(\chi)}\right)^2\right]^{1/2}.$$

Since this turns out to be only 18%, the equation for q,

$$q/e = n_v(1/\epsilon + \tfrac{1}{3}f_c) \tag{9}$$

gives a good account of the magnitude of the bond charge.

Even though we have carefully avoided highly ionic crystals, so as to maximize the validity of Eq. (6), a significant part of the 18% deviation we found is probably still due to the inadequacy of this simple equation of motion. Thus, it seems reasonable to conclude that Eq. (9) may be more accurate than this 18% deviation would indicate. Since q only enters linearly into the calculation of the nonlinear susceptibility, this will be satisfactory for our purposes.

TABLE I. Comparison between the bond charge $q(\chi)$ determined from the susceptibility [i.e., Eqs. (8)] and q(calc) determined from Eq. (9).

Crystal	$q(\chi)/e$	q(calc)$/e$
C	0.831	1.018
Si	0.623	0.833
Ge	0.618	0.792
Sn	0.555	0.750
SiC	0.786	0.840
BN	0.896	0.935
BP	0.726	0.872
BAs	0.701	0.845
AlN	0.873	0.787
AlP	0.743	0.671
AlAs	0.758	0.623
AlSb	0.720	0.574
GaN	0.882	0.736
GaP	0.730	0.668
GaAs	0.715	0.640
GaSb	0.660	0.629
InN	0.863	0.653
InP	0.738	0.594
InAs	0.704	0.590
InSb	0.658	0.575

Fortunately, in our calculation of the nonlinear susceptibility we do not need to know the bond-charge equation of motion, since all we really require is an expression for the linear susceptibility. The Phillips[37] and Van Vechten[38] (PV) theory of the linear susceptibility is admirably suited for our calculations; since it is in agreement with experiment for χ (by construction), it gives an excellent account of the ionicity, and is a macroscopic theory which automatically includes the potentially troublesome local field correctly. Because we can thus calculate the macroscopic *nonlinear* susceptibility using bond parameters (e.g., f_i, q) determined, essentially self-consistently, from the macroscopic *linear* susceptibility, we are able to obtain accurate values for d_{ijk}.

It is instructive to compare the microscopic Eqs. (8) with the macroscopic PV expression

$$\chi = \frac{1}{4\pi}\,\frac{(\hbar\Omega_p)^2}{E_g^2}\,, \qquad (\hbar\Omega_p)^2 = (4\pi Ne^2/m)\,DA\,, \tag{10}$$

where D and A are correction factors of order unity. Equating Eqs. (8) and (10) shows

$$(\hbar\Omega_p)^2 = (\hbar\omega_q)^2 f. \tag{11}$$

TABLE II. Comparison between the theoretical and experimental ratios of d_{ijk} coefficients. The theoretical result assumes undistorted tetrahedra.

Crystal (II-VI)	$(d_{31}/d_{33})_{\text{expt}}$	$(d_{15}/d_{33})_{\text{expt}}$
ZnS[a,b]	−0.51	−0.56
CdS[a,c,d]	−0.55	−0.60
CdSe[a,e]	−0.53	−0.58
Theory: $d_{31}/d_{33}=d_{15}/d_{33}=-\frac{1}{2}$		

[a]C. K. N. Patel, Phys. Rev. Letters 16, 613 (1966).
[b]R. C. Miller, S. C. Abrahams, R. L. Barns, J. L. Bernstein, W. A. Nordland, and E. H. Turner, Solid State Commun. 9, 1463 (1971).
[c]R. C. Miller, D. A. Kleinman, and A. Savage, Phys. Rev. Letters 11, 146 (1963); R. A. Soref and H. W. Moos, J. Appl. Phys. 35, 2152 (1964).
[d]R. C. Miller and W. A. Nordland, Phys. Rev. B 2, 4896 (1970).
[e]R. C. Miller and W. A. Nordland, Phys. Rev. B 5, 4931 (1972).

This shows that the macroscopically defined plasma frequency $\hbar\Omega_p$ of PV, which is in excellent agreement with experiment, implicitly contains the local-field factor f. Hence Eq. (10) is an attractive starting point for our calculation of the nonlinear susceptibility, as it avoids these complications. This is especially important, since these local-field effects are a much larger source of error in the nonlinear susceptibility ($d_{ijk}\propto f^3$) than in the linear susceptibility ($\chi\propto f$).

III. LINEAR SUSCEPTIBILITY

We will now discuss in detail the various parameters appearing in Phillips[37] and Van Vechten's[38] expression for the linear susceptibility [Eqs. (10)] and their dependence on the microscopic variables r_α (the covalent radius), Z_α (the core charge), and the other relevant variables. Although PV only considered the simple AB compounds, I have already discussed in some detail (Refs. 1 and 2, hereafter referred to as I and II) the extention of these ideas to a wide variety of complex multibond crystals, and simply exhibit the results of this generalization in what follows.

If the crystal is composed of different types of bonds (labeled μ), then the total χ can be resolved into contributions χ^μ from the various types of bonds,

$$\chi=\sum_\mu F^\mu\chi^\mu=\sum_\mu N_b^\mu\chi_b^\mu\,, \tag{12}$$

where χ^μ is the total macroscopic susceptibility which a single crystal composed entirely of bonds of type μ would have (including local-field effects), F^μ is the fraction of bonds of type μ composing the actual crystal, χ_b^μ is the macroscopic susceptibility of a single bond of type μ, and N_b^μ is the number of bonds per cm^3. In terms of more fundamental variables

$$\chi^\mu=\frac{1}{4\pi}\,\frac{(\hbar\Omega_p^\mu)^2(1+\Gamma^\mu)}{(E_g^\mu)^2}\,. \tag{13}$$

Equation (13) defines the appropriate average energy gap for the type-μ bonds, E_g^μ, and Γ describes the effects of conduction-band d levels ($\Gamma=0$ if there are no such d levels).

The plasma frequency Ω_p^μ is obtained from the number of valence electrons of type μ per cm^3, N_e^μ using

$$(\hbar\,\Omega_p^\mu)^2=(4\pi N_e^\mu e^2/m)D^\mu A^\mu\,, \tag{14}$$

where D^μ and A^μ are correction factors of order unity.[38]

It is useful to express N_e^μ in terms of individual bond properties

$$N_e^\mu=n_v^\mu/v_b^\mu\,, \tag{15a}$$

$$n_v^\mu=(Z_\alpha^\mu/N_{c\alpha}^\mu+Z_\beta^\mu/N_{c\beta}^\mu)\,, \tag{15b}$$

where n_v^μ is the number of valence electrons per μ bond, $N_{c\alpha}^\mu$ is the coordination number of the α atom composing the μth bond, and v_b^μ is the bond volume.

In order to determine the ionicity f_i^μ and covalency f_c^μ of the individual bonds, we separate $(E_g^\mu)^2$ into homopolar $(E_h^\mu)^2$ and heteropolar $(C^\mu)^2$ parts

$$(E_g^\mu)^2=(E_h^\mu)^2+(C^\mu)^2 \tag{16}$$

and

$$f_i^\mu=(C^\mu)^2/(E_g^\mu)^2\,,\quad f_c^\mu=(E_h^\mu)^2/(E_g^\mu)^2\,. \tag{17}$$

Our generalized expressions for the evaluation of E_h^μ and C^μ in an A_mB_n compound are

$$E_h^\mu=\frac{39.74}{(d^\mu)^s}\propto\frac{1}{(r_0^\mu)^s}\,,\quad s=2.48 \tag{18}$$

$$C^\mu=b^\mu e^{-k_s^\mu r_0^\mu}\left(\frac{Z_\alpha^\mu}{r_\alpha^\mu}-\frac{n}{m}\,\frac{Z_\beta^\mu}{r_\beta^\mu}\right)e^2\,, \tag{19}$$

$$r_\alpha^\mu\simeq r_\beta^\mu\simeq r_0^\mu\equiv\tfrac{1}{2}(r_\alpha^\mu+r_\beta^\mu)=\tfrac{1}{2}d^\mu\,, \tag{20}$$

where d^μ is the bond length, r_α is the atomic radius, and $e^{-k_s r_0}$ is the Thomas–Fermi screening factor.

The physical interpretation of Eq. (19) is that the antisymmetric energy gap C^μ is given by the difference between the screened Coulomb potentials of the atoms α and β (having core charges Z_α^μ and Z_β^μ) composing the bond μ. As shown in I and II, the implicit dependence of b on the covalent radii[43] (the position of the bond charge) is such that superior results for the linear dielectric properties are obtained by using $r_\alpha\simeq r_\beta$ [except when $Z_\alpha/Z_\beta\simeq(mr_\alpha)/(mr_\beta)$].

The d electrons in noble- or transition-metal atoms are weakly bound and consequently give sizable effects. As shown in I and II, these impor-

tant effects can be accounted for by including all the d electrons when calculating Ω_p, i.e., N_e (e.g., $N_e = 18$ for CuCl), and also when evaluating Z_α (e.g., $Z_\alpha = 11$ for Cu). More specifically it was shown[1,2] that the ionic gap for such compounds can be represented by

$$C = b^\mu e^{-k_s^\mu r_0^\mu}\left(\frac{Z_\alpha^{\mu\,*}}{r_0^\mu} - \frac{n}{m}\frac{Z_\beta^\mu}{r_0^\mu}\right)e^2 , \tag{21}$$

where the effective noble- or transition-metal core charge Z_α^* can be determined directly from Eq. (21) [in fact $Z_\alpha^* = Z_\alpha(be^{-kr}/S)$, where S is the noble- or transition-metal screening factor]. It should be noted that Eq. (21) has been written so that the Thomas–Fermi screening factor e^{-kr} is evaluated using only the s and p electrons, since the d electrons have already been included in Z_α^*.

We found[1,2] that this prescreening factor b was quite constant within any crystal class (e.g., $b = 1.62 \pm 14\%$ for zinc blende, wurtzite) and that the differing values in the various crystal classes could be predicted quite closely by

$$b = 0.089(\bar{N}_c)^2 . \tag{22}$$

For transition-metal bonds (TMB) this b value should be multiplied by the factor containing Γ given as follows:

$$b(\mathrm{TMB}) = 0.089(\bar{N}_c)^2\left(\frac{1+\Gamma}{1-\Gamma f_c/f_t}\right)^{1/2} , \tag{23}$$

where Γ is the fractional number of conduction-band d levels. The average coordination number $\bar{N}_c$ for A_mB_n compounds is given by

$$\bar{N}_c = \left(\frac{m}{m+n}\right)N_c(A) + \left(\frac{n}{m+n}\right)N_c(B) , \tag{24}$$

where $N_c(A)$ is the coordination number of atom A.

We have already generalized the PV results for the linear susceptibility to complex multibond crystals.[1,2] All that now remains to be done before we can use these results for the nonlinear susceptibility is to generalize the symmetric potential E_h. Although Eq. (18) gives good results for the linear susceptibility, the nonlinear susceptibility is more sensitive to the crystal potentials, and hence a more accurate microscopic description is necessary.

E_h is incorrectly evaluated at the average radius r_0 and not the true bond-charge positions r_α and r_β. This is easily seen since Eq. (18) states that E_h is constant throughout the bonding region, whereas one would expect E_h to be a function of the position of the bond charge as is the case for C. In other words, although the numerical value for E_h used by PV [i.e., Eq. (18)] is very accurate, to obtain d_{ijk} we need the correct functional dependence of E_h on r_α and r_β in order to determine its variation with electric field. We now generalize the symmetric gap to include this r_α, r_β dependence. Of course since E_h must be symmetric in α and β this correction must depend on $(r_\alpha - r_\beta)^2$. However, Eq. (18) is satisfactory for the linear susceptibility since, for this case, the correction is of second order in the small quantity $(r_\alpha - r_\beta)$. On the other hand, as we will see, the nonlinear susceptibility is more sensitively dependent on the crystal potentials, and this correction factor is a first-order effect.

The contribution of atom α to E_h^2 denoted by $(E_h^2)_\alpha$ is given by generalizing Eq. (18),[33] i.e.,

$$(E_h^{-2})_\alpha \propto (r_\alpha - r_c)^{2s} , \tag{25}$$

where r_c is the appropriate core radius. The quantity r_c must be included since the valence-electron wave functions are orthogonal to those of the core. Therefore, the probability of finding a valence electron in the core region is small, and this makes the effective bond length shorter. Equation (25) is a simple way of including this important effect.

This core radius r_c does not enter in the semiclassical electrostatic expression for the ionic gap [Eq. (19)] since the Coulomb potential of a sphere of charge of radius r_c can be taken to act at its center and thus is independent of r_c. For the quantum-mechanical covalent gap, this is not the case. We will treat this core correction in a simple fashion since the fine details of the core region are not expected to affect the susceptibility in a significant way. In conformity with our use of average bond properties (e.g., the average band gap E_g), and consistent with the expectation that larger atoms have larger cores, we determine an average core radius from

$$r_c^\mu \propto r_0^\mu . \tag{26}$$

The proportionality constant may be obtained from the covalent-radii and core-radii table of Van Vechten and Phillips.[43] An average of the ratio of core radii to covalent radii, for all the atoms in Table I of VP,[43] shows that the average core radius is 35% of the average covalent radius. Thus in Eq. (26)

$$r_c^\mu = 0.35\, r_0^\mu . \tag{27}$$

To derive the dependence of the total average gap E_h^2 on the individual gaps $(E_h^2)_\alpha$ and $(E_h^2)_\beta$, we consider the average homopolar susceptibility $(\chi_h)_{\mathrm{av}}$ that the bond charge experiences, namely,

$$(\chi_h)_{\mathrm{av}} = \frac{1}{4\pi}\frac{(\hbar\Omega_p)^2}{E_h^2} . \tag{28}$$

Both atoms α and β will contribute to this average susceptibility and since susceptibilities are directly additive we have[33]

$$(\chi_h)_{\mathrm{av}} = \tfrac{1}{2}[(\chi_h)_\alpha + (\chi_h)_\beta] . \tag{29}$$

Generalizing Eq. (28) to

$$(\chi_h)_\alpha = \frac{1}{4\pi}\frac{(\hbar\Omega_p)^2}{(E_h^2)_\alpha}, \tag{30}$$

we obtain

$$E_h^{-2} = \tfrac{1}{2}[(E_h^{-2})_\alpha + (E_h^{-2})_\beta]. \tag{31}$$

Finally the combination of Eqs. (25) and (31) results in[33]

$$E_h^{-2} \propto (r_\alpha - r_c)^{2s} + (r_\beta - r_c)^{2s}, \tag{32}$$

or

$$E_h^{-2} = (E_h^{-2})_0 \frac{(r_\alpha - r_c)^{2s} + (r_\beta - r_c)^{2s}}{2(r_0 - r_c)^{2s}}, \tag{33}$$

where $(E_h^{-2})_0$ is the gap appropriate to $r_\alpha = r_\beta = r_0$, i.e., the PV gap given by Eq. (18). With these relations for the potentials in the bonding region as well as the explicit dependence of the linear susceptibility on these potentials, we can calculate the nonlinear susceptibility.

IV. DERIVATION OF d_{ijk}

We have previously described the linear χ as arising from the motion of the bond charge q under the influence of the symmetric and antisymmetric potentials E_h and C. The nonlinear optical susceptibility d_{ijk} arises from the total acentricity produced by these potentials. That is, because q is situated in an asymmetric potential, a dc electric field $\mathcal{E}$ which causes a displacement of q by Δr produces a change in the average potential. This makes the energy gap $E_g(\mathcal{E})$, and therefore also the susceptibility $\chi(\mathcal{E})$, field dependent. As we will see later the coefficient describing this electric field dependence of χ is the nonlinear optical susceptibility d_{ijk}.

We will now determine $\chi(\mathcal{E})$ by starting with Eq. (13) for the μth type of bond. As discussed previously [Eq. (11)], this formulation automatically includes most of the local-field effects, since it uses the macroscopic measured susceptibility χ^μ. For the present we take $\mathcal{E}$ parallel to ξ, where ξ is the bond direction. For one bond

$$P^\mu = \chi_b^\mu \mathcal{E} = q^\mu \Delta r^\mu, \tag{34}$$

where χ_b^μ is the linear susceptibility parallel to ξ. It should be noted that q is not necessarily a point charge, nor even spherical; all that Eq. (34) requires is that q move rigidly in response to $\mathcal{E}$. This displacement Δr^μ will produce a change in both $E_h(\Delta E_h)$ and $C(\Delta C)$ causing χ^μ to change by $\Delta\chi^\mu$. From Eq. (13) we can write for one bond

$$\Delta\chi^\mu = -\frac{\chi_b^\mu}{(E_g^\mu)^2}[\Delta(E_h^\mu)^2 + \Delta(C^\mu)^2]. \tag{35}$$

Thus, we see from Eq. (35) that the $\mathcal{E}$ dependence of both the symmetric and antisymmetric potentials are important.[33] In deriving Eq. (35) we have used the fact that d^μ remains constant, i.e.,

$$\Delta d^\mu = \Delta r_\alpha^\mu + \Delta r_\beta^\mu = 0, \tag{36}$$

so that $(\Omega_p^\mu)^2 \propto (d^\mu)^{-3}$ is also constant. Differentiating Eq. (19) with respect to r_α, we obtain

$$\Delta C^\mu = \frac{\partial C^\mu}{\partial r^\mu}\Delta r_\alpha^\mu = -b^\mu e^{-k_s^\mu r_0}[Z_\alpha^\mu + (n/m)Z_\beta^\mu]\frac{\Delta r_\alpha^\mu}{(r_0^\mu)^2}e^2. \tag{37}$$

Since the prescreening factor b is a constant within a given crystal class,[1,2,37,38] and since the Thomas-Fermi screening constant $e^{-k_s^\mu r_0}$ depends on d^μ (and not r_α) they remain unchanged when $\mathcal{E}$ is applied.

The use of Eq. (34) gives the electric field dependence of C^μ, which is

$$\Delta C^\mu = -4b^\mu e^{-k_s^\mu r_0^\mu}[Z_\alpha^\mu + (n/m)Z_\beta^\mu]\frac{(\chi_b^\mu)e^2\mathcal{E}}{q^\mu(d^\mu)^2}. \tag{38}$$

By an analogous argument, Eq. (33) yields

$$\Delta E_h^2 = -sE_h^2\frac{(r_\alpha - r_c)^{2s-1} - (r_\beta - r_c)^{2s-1}}{(r_0 - r_c)^{2s}}\Delta r_\alpha, \tag{39}$$

where for simplicity we have dropped the subscript 0 on $(E_h)_0$. Defining ρ by

$$r_\alpha^\mu = r_0^\mu(1+\rho), \qquad r_\beta^\mu = r_0^\mu(1-\rho^\mu)$$

so that

$$\rho^\mu = \frac{(r_\alpha^\mu - r_\beta^\mu)}{(r_\alpha^\mu + r_\beta^\mu)}, \tag{40}$$

and using Eq. (34) again, we find

$$\Delta E_h^2 = -4s(2s-1)\left(\frac{r_0^\mu}{r_0^\mu - r_c^\mu}\right)^2\frac{(E_h^\mu)^2\chi_b^\mu\rho^\mu\mathcal{E}}{d^\mu q^\mu}, \tag{41}$$

where for simplicity higher-order terms of order ρ^3 are neglected. Equations (38) and (41) substituted in Eq. (35) yield

$$\Delta\chi_{\xi\xi}^\mu = +\frac{8b^\mu e^{-k_s^\mu r_0^\mu}[Z_\alpha^\mu + (n/m)Z_b^\mu](\chi_b^\mu)^2 C^\mu e^2\mathcal{E}_\xi}{(E_g^\mu)^2(d^\mu)^2 q^\mu} + \frac{4s(2s-1)[r_0^\mu/(r_0^\mu - r_c^\mu)]^2 f_c^\mu(\chi_b^\mu)^2\rho^\mu\mathcal{E}_\xi}{d^\mu q^\mu}, \tag{42}$$

where the subscripts ξ on $\Delta\chi_{\xi\xi}$ and $\mathcal{E}_\xi$ remind us that this is the change in polarizability parallel to the bond axis ξ for a field applied along ξ.

All that is now necessary is to relate this change $\Delta\chi_{\xi\xi}$ to the longitudinal second-harmonic coefficient $\beta_{\xi\xi\xi}$ of the bond. One way of doing this is to begin by relating $\Delta\chi_{\xi\xi}$ to the longitudinal electro-optic coefficient $r_{\xi\xi\xi}$, which is defined by

$$r_{\xi\xi\xi}^\mu\mathcal{E}_\xi = \Delta(1/\epsilon_{\xi\xi}^\mu) = -4\pi\Delta(\chi_b^\mu)_{\xi\xi}/(\epsilon_{\xi\xi}^\mu)^2. \tag{43}$$

The second-harmonic coefficient can be expressed in terms of the electro-optic constant (in esu units[44]) by[45]

$$\beta^{\mu}_{\xi\xi\xi} = -\tfrac{1}{4}(\epsilon^{\mu}_{\xi\xi})^2 r^{\mu}_{\xi\xi\xi}/4\pi\,, \tag{44}$$

and so

$$\beta_{\xi\xi\xi} = \tfrac{1}{4}\Delta(\chi^{\mu}_{b})_{\xi\xi}/\mathcal{E}_{\xi}\,. \tag{45}$$

Because the factors of two[46] in these definitions can be confusing, we illustrate the general derivation of Eq. (45) with an explicit example in the Appendix.

Now that we have the longitudinal nonlinearity of a single bond, we want to obtain the full macroscopic tensor expression for d_{ijk}. Thus, we must now consider the transverse nonlinear susceptibility of a bond $\beta_{\perp}$. For example we might consider $\beta_1 = \beta_{\xi\eta\eta}$ (which by Kleinman[47] symmetry is also equal to $\beta_{\eta\xi\eta}$ and $\beta_{\eta\eta\xi}$), where η is the transverse direction. Since a displacement $\Delta\eta$ does not change r_{α} or r_{β} to first order, it cannot change either C^{μ} or E^{μ}_{h} to first order. The lowest-order term arising from a transverse displacement gives a term $\Delta\chi(\mathcal{E}) \propto \mathcal{E}^2$ or $P \propto \mathcal{E}^3$, which is a contribution to the third-order nonlinear susceptibility. Thus in our model we have the simple result that

$$\beta_{\perp} = 0\,. \tag{46}$$

Quantum mechanically $\beta_{\perp} \simeq 0$ because the formation of covalent bonds mainly changes the atomic wave functions along the bond; in the perpendicular direction the wave functions remain similar to those in the free atom, i.e., essentially centrosymmetric. Equation (46) is in agreement with the molecular orbital calculations of Flytzanis and Ducuing.[14]

We can now express the full macroscopic tensor nonlinear susceptibility of the entire crystal d_{ijk} as

$$d_{ijk} = \sum_{\mu} F^{\mu} d^{\mu}_{ijk} = \sum_{\mu} G^{\mu}_{ijk} N^{\mu}_{b} \beta^{\mu}_{\xi\xi\xi} \tag{47}$$

or

$$\beta^{\mu} = F^{\mu} d^{\mu}_{ijk} / G^{\mu}_{ijk} N^{\mu}_{b}\,, \tag{48}$$

where d^{μ}_{ijk} is the total macroscopic nonlinearity which a crystal composed entirely of bonds of type μ would have and F^{μ} is the fraction of bonds of type μ composing the actual crystal [this is quite analogous to the bond separation of the linear susceptibility, i.e., Eq. (12)]. Because $\beta_{\perp} = 0$ [i.e., Eq. (46)], the geometrical factor G_{ijk} can simply be calculated from

$$G^{\mu}_{ijk} = \frac{1}{n^{\mu}_{b}} \sum_{\lambda} \alpha^{\mu}_{i}(\lambda)\alpha^{\mu}_{j}(\lambda)\alpha^{\mu}_{k}(\lambda)\,, \tag{49}$$

where the sum on λ is over all n^{μ}_{b} bonds of type μ in the unit cell, and $\alpha^{\mu}_{i}(\lambda)$ is the direction cosine with respect to the ith coordinate axis of the λth bond of type μ in the unit cell. We can see that Eq. (49) automatically satisfies Kleinman symmetry[47] (i.e., complete permutation symmetry of the indices i, j, and k). The reason for this is that we have neglected any dispersion in the susceptibilities. The complete expression for the total nonlinear susceptibility can now be written as

$$d_{ijk} = \sum_{\mu} F^{\mu}[d^{\mu}_{ijk}(C) + d^{\mu}_{ijk}(E_h)]\,, \tag{50}$$

$$F^{\mu} d^{\mu}_{ijk}(C) = \frac{G^{\mu}_{ijk} N^{\mu}_{b}(600) b^{\mu} e^{-k^{\mu}_{s} r^{\mu}_{0}} [Z^{\mu}_{\alpha} + (n/m) Z^{\mu}_{\beta}] |e| (\chi^{\mu}_{b})^2 C^{\mu}}{(E^{\mu}_{g})^2 (d^{\mu})^2 q^{\mu}}\,, \tag{51}$$

$$F^{\mu} d^{\mu}_{ijk}(E_h) = \frac{G^{\mu}_{ijk} N^{\mu}_{b} s(2s-1)[r^{\mu}_{0}/(r^{\mu}_{0} - r^{\mu}_{c})]^2 f^{\mu}_{c} (\chi^{\mu}_{b})^2 \rho^{\mu}}{d^{\mu} q^{\mu}}\,. \tag{52}$$

For convenience we have written the above equations so that C^{μ} and E^{μ}_{g} are in eV, the other variables are in esu, as is d_{ijk}. The value of the factor $r_0/(r_0 - r_c)$ can be obtained from Eq. (27). Note that Eqs. (47)–(52) express the nonlinear optical susceptibility in terms of known quantities, so that we do not need to fit any parameters to the *nonlinear* optical susceptibility for any crystal. In other words, the parameters b, q, χ_b, C, E_g, f_c, etc., have already been determined using only the *linear* susceptibility and the radii r_{α}. In this sense our theory does not use any adjustable parameters.

We see that there are two sources of bond acentricity: the electronegativity difference C of the atoms composing the bond which leads to $d_{ijk}(C)$, and the difference in the atomic sizes $\rho = (r_{\alpha} - r_{\beta})/(r_{\alpha} + r_{\beta})$ which leads to $d_{ijk}(E_h)$. The latter term is of course only important when the two atoms have quite different radii, as for example in a bond containing one atom from the first periodic row. The reason for this is that the homopolar gap E_h is symmetric in α and β so that $\partial E_h/\partial r_{\alpha}$ vanishes by symmetry for $r_{\alpha} = r_{\beta}$. Actually, when ρ is as small as ~ 0.1, it is not really significantly different from zero to within the uncertainties involved in the determination[43,48] of r_{α}. This means that for small ρ's, say, $\rho \simeq 0.05$, a change in r_{α} by only 4% (keeping d constant) can change ρ by as much as a factor of 5. Hence, for simplicity we will take

$$\rho^{\mu} \simeq 0 \quad \text{when } \rho^{\mu} \lesssim 0.1\,. \tag{53}$$

Since Miller's[18] Δ_{ijk} is normalized to the linear susceptibility, it is more closely related to the intrinsic crystalline acentricity than d_{ijk} is, and Δ_{ijk}

is therefore a useful representation for the nonlinear susceptibility. It is defined by[18]

$$\Delta_{ijk}=\frac{d_{ijk}}{\chi_i(\omega_i)\chi_j(\omega_j)\chi_k(\omega_k)}\,, \tag{54}$$

where ω_i are the appropriate optical frequencies involved, and $\chi_i(\omega_i)$ is the appropriate susceptibility at ω_i. We can express Eqs. (47)–(52) in terms of this Δ_{ijk} formulation as

$$\Delta_{ijk}=\sum_\mu F^\mu\Delta^\mu_{ijk}=\sum_\mu G^\mu_{ijk}N^\mu_b\Delta^\mu_\beta\,, \tag{55}$$

where Δ_β is the Miller's Δ for the bond, i.e.,

$$\Delta^\mu_\beta=F^\mu\Delta^\mu_{ijk}/G^\mu_{ijk}N^\mu_b\,. \tag{56}$$

Further, we have

$$\Delta_{ijk}=\sum_\mu F^\mu[\Delta^\mu_{ijk}(C)+\Delta^\mu_{ijk}(E_h)]\,, \tag{57}$$

$$F^\mu\Delta^\mu_{ijk}(C)=\frac{G^\mu_{ijk}N^\mu_b(600)b^\mu e^{-k^\mu_s r^\mu_0}[Z^\mu_\alpha+(n/m)Z_\beta]\,|e|\,(\chi^\mu_b)^2C^\mu}{(E^\mu_g)^2(d^\mu)^2q^\mu\chi^3}\,, \tag{58}$$

and

$$F^\mu\Delta^\mu_{ijk}(E_h)=\frac{G^\mu_{ijk}N^\mu_b s(2s-1)[r^\mu_0/(r^\mu_0-r^\mu_c)]^2 f^\mu_c(\chi^\mu_b)^2\rho}{d^\mu q^\mu\chi^3}\,. \tag{59}$$

In the denominators of Eqs. (58) and (59), χ is the total macroscopic susceptibility. This is convenient since then, as Eq. (57) shows, all the contributions are directly additive. It is important to note that no approximations have been made in deriving Eqs. (55)–(59) from Eqs. (47)–(52), since we have merely divided by χ^3 and redefined the nonlinearity in terms of Δ_{ijk}. This Δ_{ijk} formulation is useful since in our calculation we use the extrapolated low-frequency electronic susceptibility χ, whereas the experimentally measured nonlinearity may include a significant amount of dispersion. As is well known,[49] the effects of dispersion on Δ_{ijk} are much less pronounced than for d_{ijk}, and hence for a meaningful comparison between our theory and experiment it is appropriate to use Δ_{ijk}. To obtain a theoretical value for d_{ijk} one simply substitutes the Δ_{ijk} calculated from Eqs. (55)–(59) into Eq. (54).

It may be of interest to point out that Eqs. (55)–(59) show that a crude estimate of a typical Δ is given by

$$\Delta\simeq 1/P_q\,, \tag{60}$$

where $P_q\equiv\chi q/r_0^2$ is the atomic polarization produced by the bond-charge electric field q/r_0^2. This simple relation is instructive since it gives the correct order of magnitude for Δ and shows that Δ is given by an inverse atomic (i.e., bond charge) polarization. Taking typical values for $q/e\sim 0.6$, $d\sim 2.5$ Å, $\chi\sim\frac{1}{2}$ yields $P_q\sim 0.9\times10^6$ esu and $\Delta\sim 1.1\times10^{-6}$ esu, which is close to the average value[18] for Δ.

V. SIGN OF d_{ijk}

The absolute sign of d_{ijk} is of fundamental significance since it depends on whether the potentials in the bonding region increase or decrease with an applied electric field. In Eq. (51) the three relevant quantities which possess signs are G_{ijk}, q, and $[Z_\alpha/r_\alpha-(n/m)Z_\beta/r_\beta]$; the latter quantity comes from the factor C^μ. As an illustration let us consider, say, GaP. In this example $G_{14}=(1/\sqrt{3})^3>0$, $q<0$ (the bond charge is composed of electrons and the difference in Coulomb potentials in the brackets above is proportional to $[3-5]<0$. The product of these three quantities is therefore positive and so $d_{14}(C)>0$. Perhaps this result can be seen more graphically by returning to Eqs. (35) and (37), that is, to

$$d_{ijk}(C)\propto[Z_\alpha-(n/m)Z_\beta]\,\Delta r_\alpha\,. \tag{61}$$

Figure 1 shows that a positive electric field $\mathcal{E}$ (defined as pointing from the Ga to the P along a [111] crystallographic direction) will cause q to move in the negative direction ($q<0$) and thus $\Delta r_\alpha<0$. Since $[Z_\alpha-Z_\beta]=[3-5]<0$, we again see from Eq. (61) that $d_{14}(C)>0$ for GaP.[33]

As far as $d_{ijk}(E_h)$ is concerned, Eq. (52) shows that the three factors determining the sign are G_{ijk}, q, and ρ. Thus, since $q<0$ and $G_{33}>0$ for, say, wurtzite crystals, the sign of d_{33} is opposite to that of ρ. A positive ρ means that $r^\mu_\alpha>r^\mu_\beta$ [see Eq. (40)], i.e., the metal atom is larger than the nonmetal atom as in, say, ZnO. Consequently, $d_{33}(E_h)<0$ for ZnO.[33] Since in general $d_{ijk}(C)$ and $d_{ijk}(E_h)$ can have the same or opposite signs, interesting cancellations between these two terms leading to anomalously low nonlinearities can occur, as we will see later.

VI. TETRAHEDRAL *AB* COMPOUNDS

A. No First-Row Atoms or Noble Metals

The simplest acentric crystals are the tetrahedrally coordinated zinc-blende and wurtzite semi-

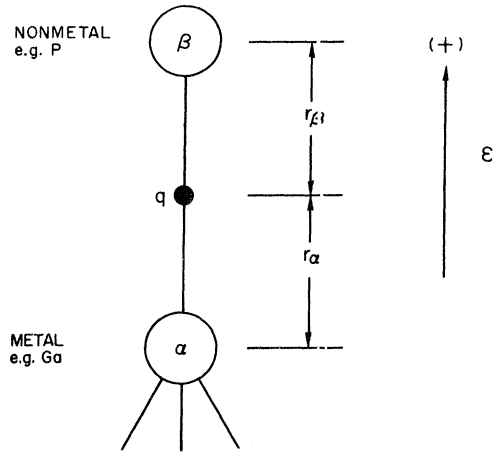

FIG. 1. Schematic representation of the bonding region, showing the bond charge q located a distance r_α and r_β from the α and β atoms. The positive electric field ($\mathcal{E}$) direction is also shown as pointing from the metal to the nonmetal (or from cation to anion). This positive direction corresponds, in say GaP, to the outward normal of the Ga terminated (111) face.

conductors containing neither a first-row element (i.e., $\rho = 0$) nor a noble metal (i.e., no strong d-electron effects). The geometrical factors, Eq. (49), for the $d_{14} \equiv d_{123}$ coefficient in zinc blende and the $d_{33} \equiv d_{333}$, $d_{31} \equiv d_{311}$, and $d_{15} \equiv d_{113}$ coefficients in wurtzite (assuming perfect tetrahedra) are

$$G_{14} = +\frac{1}{3\sqrt{3}} \quad \text{(zinc blende)},$$
$$G_{33} = +\tfrac{2}{9}, \quad G_{31} = G_{15} = -\tfrac{1}{9} \quad \text{(wurtzite)}. \tag{62}$$

These geometrical factors were first derived by Robinson.[25] As a check on our assumption that the bonds can be treated *independently*, i.e., that the bond-bond interactions can be assumed negligible (or assumed to be already included by our use of the measured macroscopic susceptibility), we can compare the predicted ratio of $d_{31}/d_{33} = -\frac{1}{2}$ [from Eq. (49)] with experiment. This is done in Table II, where this prediction is seen to be quite accurate, supporting our independent bond model.

Using these geometrical factors, together with Eqs. (54)–(59) and the known[1,38,50] linear properties of these crystals results in the nonlinear coefficients listed in Table III. The experimental agreement is excellent in both magnitude and sign and is achieved without the benefit of any adjustable parameters.

The good result for InSb is especially interesting in view of its extremely small minimum gap $E_0 = 0.24$ eV. That is, one might expect that since E_0 is more than an order of magnitude smaller than $E_g = 3.8$ eV, the Γ point of the Brillouin zone would make a significant contribution to d_{ijk}. Our good experimental agreement shows that these Γ-point contributions are implicitly included in our use of the measured macroscopic susceptibility and our treatment of the local-field problem. Also, our localized real-space picture, being a Fourier transform over k space, does include contributions from various points in the Brillouin zone.

In order to better exhibit the interesting dependence of d_{ijk} on the fundamental variables ΔZ and d, we can plot Eq. (51) as a function of d for con-

TABLE III. Comparison between theoretical $\Delta_{ijk}^{\text{calc}}$ and experimental $\Delta_{ijk}^{\text{expt}}$ nonlinearities. The numbers in parentheses next to the crystals [(14) or (33)] refer to the tensor components ijk. The numbers in parentheses next to the Δ_{ijk} values are for $|d_{ijk}^{\text{calc}}|$ and $|d_{ijk}^{\text{expt}}|$ in units of 10^{-9} esu. The d_{ijk} values of ZnS and CdS are for 1.06 μ, that of InSb is the extrapolated long-wavelength value, and the other crystals are for 10.6 μ. Conversion from relative to absolute nonlinearities was done using Ref. 77.

Crystal	$\Delta_{ijk}^{\text{calc}}$ (10^{-9} esu)	$\Delta_{ijk}^{\text{expt}}$ (10^{-9} esu)
III-V		
AlP (14)	+0.68	
AlAs (14)	+0.73	
AlSb (14)	+0.76	
GaP (14)	+0.54 (130)	+0.41[a,b] (99)
GaAs (14)	+0.49 (230)	+0.46[a,b] (215)
GaSb (14)	+0.42 (520)	+0.52[b] (650)
InP (14)	+0.71	
InAs (14)	+0.56 (410)	+0.59[b] (430)
InSb (14)	+0.50 (790)	± 0.56[c] (870)
II-VI		
ZnS (33)	+1.27 (55)	+1.04[a,d] (45)
ZnSe (14)	+1.12 (65)	≃+0.9[e,f]
ZnTe (14)	+1.12 (138)	≃+1.1[e,g,h]
CdS (33)	+1.54 (95)	+1.10[i,f] (68)
CdSe (33)	+1.56 (99)	+1.36[j,h] (86)
CdTe (14)	+1.39 (173)	+[h]

[a]B. F. Levine and C. G. Bethea, Appl. Phys. Letters 20, 272 (1972).

[b]J. J. Wynn and N. Bloembergen, Phys. Rev. 188, 1211 (1969).

[c]S. S. Jha and J. J. Wynn, Phys. Rev. B 5, 4867 (1972).

[d]R. C. Miller, S. C. Abrahams, R. L. Barns, J. L. Bernstein, W. A. Nordland, and E. H. Turner, Solid State Commun. 9, 1463 (1970).

[e]R. A. Soref and H. W. Moos, J. Appl. Phys. 35, 2152 (1964).

[f]R. C. Miller and W. A. Nordland, Phys. Rev. B 2, 4896 (1970).

[g]R. K. Chang, J. Ducuing, and N. Bloembergen, Phys. Rev. Letters 15, 415 (1965).

[h]R. C. Miller and W. A. Nordland, Phys. Rev. B 5, 4931 (1972).

[i]R. C. Miller, Appl. Phys. Letters 5, 17 (1964), and private communication.

[j]G. D. Boyd, E. Buehler, and F. G. Storz, Appl. Phys. Letters 18, 301 (1971).

stant $\Delta Z = 2$ and 4. Unfortunately, in order to do this we cannot use the experimental values for χ since we must calculate χ in order to exhibit the full dependence of Eq. (51) on d. Thus, the resulting theoretical curves (shown in Fig. 2) will not be as accurate as the calculation given in Table III (which uses the correct experimental χ), and are only given to exhibit the trends in d_{ijk} more clearly. There is a rather dramatic increase of d_{ijk} with d, which is mostly due to the increasing linear susceptibility (caused by the decrease in E_g). Another striking feature of Fig. 2 is the fact that d_{ijk} for $\Delta Z = 4$ crystals is lower than that for $\Delta Z = 2$. This is due to the larger band gap E_g for the more ionic $\Delta Z = 4$ crystals causing the linear and nonlinear susceptibilities to decrease.

We can better exhibit this decrease of d_{ijk} with ΔZ, i.e., ionicity, by rewriting Eq. (51). By making several approximations we can show that a rough estimate of the nonlinearity is given by

$$d_{ijk}/d^6 = 5.5\times10^{-9}[f_i(1-f_i)^5]^{1/2}\ \text{esu}, \qquad (63)$$

where d is in Å. This relation is plotted in Fig. 3, where it can be seen that there is a maximum in (d_{ijk}/d^6) for $f_i = \frac{1}{6}$, as noted previously by others.[14,17] Thus, for a large nonlinearity it is desirable to have a long bond length d (as also shown in Fig. 2), and also an ionicity which is neither too large nor too small.

The origin of this maximum can be seen from the relation $d_{ijk} = \Delta_{ijk}\chi^3$. As f_i increases Δ_{ijk} also increases and hence d_{ijk} initially increases. However, for large ionicities ($f_i > \frac{1}{6}$), χ^3 is decreasing far more rapidly than Δ_{ijk} is increasing, thus producing a maximum.

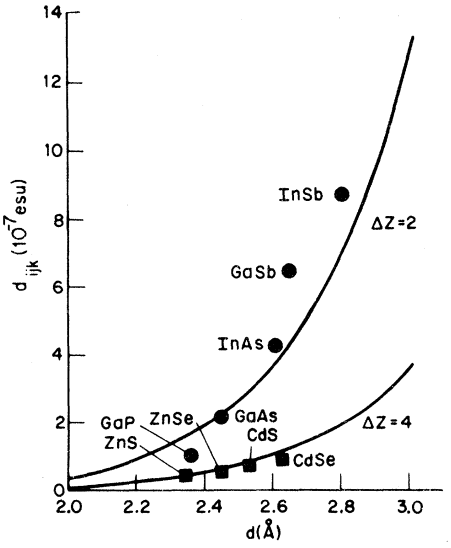

FIG. 2. Plot for the simple AB compounds, illustrating the strong dependence of the nonlinear susceptibility d_{ijk} on the bond length d, and the valence difference ΔZ. The curves are approximate theoretical expressions; the points are experiment.

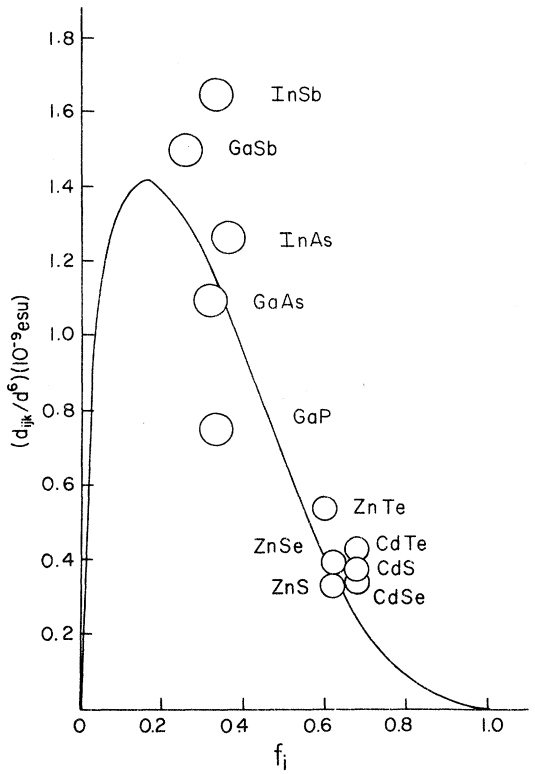

FIG. 3. Plot for the simple AB compounds, illustrating the initial increase and then decrease of the nonlinear optical susceptibility with ionicity. The circles are calculated from Eq. (51), while the curve is an approximate simplification of this equation, i.e., $(d_{ijk}/d^6) = 5.5\times10^{-9}[f_i(1-f_i)^5]^{1/2}$ esu (where d is in Å). Note the interesting maximum at $f_i = \frac{1}{6}$.

B. First-Row Atoms

For crystals containing a first-row atom the difference in atomic sizes[43] can be pronounced and ρ can be quite large ($\rho \simeq 0.2$–0.3); hence the second term in Eqs. (57) and (50), i.e., $\Delta_{ijk}(E_h)$ or $d_{ijk}(E_h)$, becomes important.[33] Since the two terms in Eq. (57) or (50) may be of comparable magnitude but opposite sign, interesting cancellation effects can occur leading to anomalously small nonlinearities. The two contributions to the nonlinearity as well as the total calculated nonlinear susceptibility are exhibited in Table IV, and compared with experiment. Note that the negative signs of d_{33} in both BeO and ZnO are correctly obtained and arise from the negative size contribution being larger than the positive electronegativity (or ionicity) term. The situation in BeO is particularly interesting as the two acentricity contributions nearly cancel[33] leading to an anomalously small

TABLE IV. Comparison between theoretical Δ_{33}^{calc} and experimental Δ_{33}^{expt} Miller's Δ's. The numbers in parentheses next to the Δ values are for $|d_{33}^{calc}|$ and $|d_{33}^{expt}|$ in units of 10^{-9} esu measured at 1.06 μ. Conversion from relative to absolute nonlinearities was done using Ref. 77.

Crystal	ρ	$F^{\mu}\Delta_{ijk}^{\mu}(C)$ (10^{-6} esu)	$F^{\mu}\Delta_{ijk}^{\mu}(E_h)$ (10^{-6} esu)	Δ_{ijk}^{calc} (10^{-6} esu)	Δ_{ijk}^{expt} (10^{-6} esu)
III-V					
AlN (33)	+0.293	+0.71	−2.02	−1.31	
GaN (33)	+0.260	+0.70	−1.73	−1.03	
InN[a] (33)	+0.323	+0.84	−2.27	−1.43	
II-VI					
BeO (33)	+0.180	+0.83	−1.07	−0.24 (0.90)	−0.13[b,c] (0.50)
ZnO (33)	+0.287	+1.08	−1.94	−0.86 (11)	−0.19[c,d] (15)

[a]No experimental dielectric data are available, and it has been estimated theoretically (Ref. 1).

[b]J. Jerphagnon and H. W. Newkirk, Appl. Phys. Letters 18, 245 (1971).

[c]R. C. Miller and W. A. Nordland, Phys. Rev. B 2, 4896 (1970).

[d]R. C. Miller, Appl. Phys. Letters 5, 17 (1964), and private communication.

Miller Δ (i.e., approximately an order of magnitude lower than usual). It should be noted that, owing to the close cancellation, the agreement between theory and experiment is better than it appears to be, being really quite good; e.g., a decrease of $\Delta(E_h)$ by only 10% is required to get coincidence between the two [obviously coincidence can be achieved with only a 5% variation of both $\Delta(C)$ and $\Delta(E_h)$]. For ZnO a 15% increase of $\Delta(E_h)$ will give coincidence between theory and experiment. Clearly, in a search for materials with large nonlinearities for practical devices, such cancellations, should be avoided.

We now turn to a consideration of the tensor character of the nonlinearity. As demonstrated in Table V, the ratios d_{31}/d_{33} and d_{15}/d_{33} deviate significantly from the theoretical expectation of $-\frac{1}{2}$. The reason that these $\rho \neq 0$ crystals are worse than the $\rho = 0$ compounds (for which the theoretical expectations are well satisfied) is related to the partial cancellation between the positive and negative $d_{33}(C)$ and $d_{33}(E_h)$ contributions. Small distortions from the assumed perfect tetrahedra will thus affect the total d_{33} more strongly. Actually for ZnO the cancellation is not extreme, and hence the ratios are still in reasonable agreement with theoretical predictions based on perfect tetrahedra. However, for BeO the cancellation is nearly complete with the total nonlinear coefficient being approximately an order of magnitude smaller than usual. Thus, the sensitivity to tetrahedra distortions is roughly an order of magnitude larger, which is apparently sufficient to invalidate the simple geometrical argument $d_{31}/d_{33} = d_{15}/d_{33} = -\frac{1}{2}$. (We will see later that there is a similar situation in $LiGaO_2$.) We can see this in more detail by considering the geometrical factors which enter into the evaluation of the various tensor elements. For the d_{33} coefficient practically all of the nonlinearity is produced by the bond parallel to the hexagonal axis; each of the other three bonds in the tetrahedron only contribute ~3% of the total. Thus, the perfection of the tetrahedral arrangement has only a rather minor influence on d_{33} since it is essentially determined by a large contribution from one bond. On the contrary, for the d_{31} or d_{15} coefficients no one bond dominates, and the nonlinearity of each of the three contributing bonds is severely reduced by a small geometrical factor equal to $\frac{4}{27} = 15\%$. For comparison the full nonlinearity (i.e., geometrical factor 100%) of the single bond parallel to the hexagonal axis is effective for d_{33}. Since the individual bond contributions to d_{31} and d_{15} are geometrically reduced by nearly an order of magnitude from their maximum possible value, it would be expected that distortion effects would be roughly an order of magnitude more important than for d_{33}. This is especially true for BeO where there is the additional close cancellation between $d_{ijk}(C)$ and $d_{ijk}(E_h)$. In summary, d_{33} is relatively insensitive to tetrahedral distortions and is therefore the quantity to be compared with theory.

TABLE V. Comparison between the theoretical and experimental ratios of d_{ijk} coefficients. The theoretical result assumes undistorted tetrahedra.

Crystal	$(d_{31}/d_{33})_{expt}$	$(d_{15}/d_{33})_{expt}$
II-VI		
BeO[a]	+0.73	
ZnO[b-d]	−0.33	−0.33
Theory: $d_{31}/d_{33} = d_{15}/d_{33} = -\frac{1}{2}$		

[a]J. Jerphagnon and H. W. Newkirk, Appl. Phys. Letters 18, 245 (1971).

[b]R. C. Miller, Appl. Phys. Letters 5, 17 (1964).

[c]R. C. Miller and W. A. Nordland, Appl. Phys. Letters 16, 174 (1970).

[d]R. C. Miller and W. A. Nordland, Phys. Rev. B 2, 4896 (1970).

C. Noble-Metal Atoms

Owing to the weak binding energy of the noble-metal d electrons, they play an important role in influencing a number of physical properties (see II and Ref. 34, and references therein). In particular d_{14} of CuCl has a negative sign which is opposite to the other zinc-blende and wurtzite crystals not possessing a first-row atom. This sign reversal shows that the d-electron contribution to the nonlinearity is substantial.[34] The origin of this sign reversal can be directly seen from Eq. (21) where, as discussed in Refs. 2 and 34, Z_α^* includes the noble-metal d electrons ($Z_\alpha^* = 15.8$ for CuCl) so that $Z_\alpha^* > Z_\beta$ and thus $[Z_\alpha^* - Z_\beta] = [15.8 - 7] > 0$. This may be contrasted with the usual situation described in Sec. VI A in which $[Z_\alpha - Z_\beta] < 0$ (e.g., for GaP, $[3 - 5] < 0$). Thus, from Eq. (61) the sign reversal of d_{14} between CuCl ($d_{14} < 0$) and say GaP or ZnS, etc., ($d_{14} > 0$), can be understood.

In order to calculate the nonlinear coefficients of these noble-metal compounds all we need to do is replace Z_α in Eq. (58) with Z_α^* and r_c in Eq. (59) with the value appropriate to noble-metal *bonds* r_c^*. The values for most of the required parameters (e.g., Z_α^*, b, C, E_h, E_g, f_i, etc.) are given in II, the other necessary parameters are treated below.

As discussed previously[2,34] a large value for the Cu-atom-core correction factor $(r_c)_{Cu}$ is indicated by the weak binding energy for the d electrons and by their relatively delocalized character.[51-54] This delocalization is indicated by the substantial p-d hybridization[51-54] in these compounds caused by the significant overlap of the noble-metal d electrons with the anion p electrons. Consistent with the observed strong d-electron effects and the substantial delocalization, we take the largest reasonable value for $(r_c)_{Cu}$, namely,

$$(r_c)_{Cu} \simeq r_0 . \tag{64}$$

We do not take $(r_c)_{Cu}$ any larger, since it seems appropriate to have these d electrons mostly situated near the Cu atom [which is consistent with Eq. (21) in which the non-noble-metal β atom is screened only by the s and p electrons, not the d electrons]. It is noteworthy that this noble-metal-atom d-core radius in Eq. (64) is almost a factor of 3 larger than usual [i.e., Eq. (27)] and thus has a volume more than 20 times larger than "normal" (i.e., non-noble-metal) d cores. In view of the large size difference between the noble-metal core $(r_c)_{Cu}$ and the "normal" d core equal to $0.35\, r_0$ [from Eq. (27)], it is reasonable to average the atomic-core radii of the bond constituents to obtain an effective core correction factor for the bond, r_c^*, to be used in Eq. (59). That is

$$(r_c^*)_{CuX} = [(0.35 r_0)(r_c)_{Cu}]^{1/2} , \tag{65}$$

and with Eq. (64) this leads to

$$(r_c^*)_{CuX} = 0.59 r_0 . \tag{66}$$

This averaging procedure to obtain r_c^* is consistent with our averaging of all the core radii given in the Van Vechten and Phillips radii tables[43] to determine the proportionality constant in Eq. (27).

Because Ag has a somewhat larger core than Cu, we would expect $(r_c^*)_{Ag}$ to be slightly larger than indicated by Eq. (66). We can estimate the ratio of these core radii by using[43] $r_c \propto n^2/Z_{eff}(\mathrm{IV})$, where n is the Slater[55] effective principal quantum number (e.g., $n = 3$ for Cu and $n = 3.7$ for Ag), and Z_{eff} is the effective charge for the group-IV element in the same periodic row as the element in question [e.g., $Z_{eff}(\mathrm{IV}) = Z_{eff}(\mathrm{Ge}) = 20.75$ for Cu and $Z_{eff}(\mathrm{IV}) = Z_{eff}(\mathrm{Sn}) = 22.25$ for Ag]. Thus,

$$(r_c)_{Ag}/(r_c)_{Cu} = 1.42 . \tag{67}$$

From the VP radii tables[43] we find

$$(r_\alpha)_{Ag}/(r_\alpha)_{Cu} = 1.405/1.225 = 1.15 , \tag{68}$$

and therefore, the relation for Ag which is analogous to Eq. (64) for Cu can be obtained from the ratio

$$\frac{(r_c)_{Ag}/(r_\alpha)_{Ag}}{(r_c)_{Cu}/(r_\alpha)_{Cu}} \simeq 1.2 . \tag{69}$$

This by comparison with Eq. (64) gives

$$(r_c)_{Ag} \simeq 1.2 r_0 . \tag{70}$$

Substituting Eq. (70) into $(r_c^*)_{AgX} = [(0.35 r_0)(r_c)_{Ag}]^{1/2}$ [analogous to Eq. (65)] yields the final result

$$(r_c^*)_{AgX} = 0.65 r_0 ; \tag{71}$$

i.e., the effective Ag core r_c^* is ~10% larger than the Cu core [i.e., Eq. (66)].

Although, as just discussed, the noble-metal d electrons are far more delocalized than those in "normal" d cores, we found it appropriate to have these d electrons mostly situated around the noble-metal atom. Therefore, to be consistent with this partial localization, it seems reasonable that these d electrons would not participate as strongly toward the formation of the bond charge q as do the even more delocalized s and p electrons. Therefore we suggest that q be evaluated using exactly the same relation [Eq. (9)] as was used in non-d-electron materials, i.e.,

$$q/e = n_v(1/\epsilon + \tfrac{1}{3} f_c) , \tag{72}$$

where n_v is the number of s and p valence electrons. In other words, the d-electron contributions to q are already included in Eq. (72) through their significant influence on ϵ and f_c.

The only other parameters needed for the evaluation of Δ_{ijk} in the noble-metal halides are the atomic radii $r_{\alpha,\beta}$ (i.e., ρ). We note that the ionicity of these halides $f_i = 0.86$–0.89 is intermediate

between the highly ionic alkali halides [e.g., $f_i(\mathrm{NaCl}) = 0.94$] and the relatively covalent zinc-blende and wurtzite crystals not containing noble metals [e.g., $f_i(\mathrm{CdS}) = 0.68$]. Thus we would expect that the appropriate atomic radii have a value intermediate[33] between the ionic[56] and covalent radii,[43] i.e.,

$$r_{\alpha,\beta} = [(r_{\mathrm{cov}})(r_{\mathrm{ion}})]^{1/2}. \tag{73}$$

Owing to the strong influence of the d electrons on the properties of Cu, it seems slightly more accurate to determine the halogen radius r_X from Eq. (73) and then determine r_{Cu} directly from the Cu-halide bond length $d_{\mathrm{Cu}X}$, i.e.,

$$r_{\mathrm{Cu}} + r_X = d_{\mathrm{Cu}X}. \tag{74}$$

Since fluorine is the smallest halogen its use in Eq. (74) should lead to the most accurate determination of r_{Cu}. Substituting $r_{\mathrm{cov}} = 0.672$ Å[43] and $r_{\mathrm{ion}} = 1.36$ Å[56] for F in Eq. (73) yields $r_{\mathrm{F}} = 0.96$ Å. Actually this value is somewhat too large as can be seen by reference to Table II of VP.[43] In their table the bond lengths calculated from the radii are compared with experiment. The noble-metal halides CuCl, CuBr, CuI, and AgI are all in very good agreement with the measured bond lengths; the only noble-metal halide in significant disagreement is CuF, for which the calculated value is 0.06 Å too large. This is not too surprising since first-row atoms tend to behave anomalously. This suggests that F is about 0.06 Å too large and so we propose to reduce our previous estimate of $r_F = 0.96$ Å to

$$r_{\mathrm{F}} = 0.90 \text{ Å}. \tag{75}$$

Equations (74) and (75) with $d_{\mathrm{CuF}} = 1.84$ Å yield

$$r_{\mathrm{Cu}} = 0.94 \text{ Å}. \tag{76}$$

We can now employ Eqs. (74) and (76) to determine

$$r_{\mathrm{Cl}} = 1.40 \text{ Å}, \tag{77a}$$

$$r_{\mathrm{Br}} = 1.52 \text{ Å}, \tag{77b}$$

$$r_{\mathrm{I}} = 1.68 \text{ Å}, \tag{77c}$$

and Eq. (77c), together with the bond length in AgI ($d = 2.80$ Å), to obtain

$$r_{\mathrm{Ag}} = 1.12 \text{ Å}. \tag{78}$$

We can now calculate Δ_{ijk} from Eqs. (55)–(59) for these noble-metal halides. The results presented in Table VI show an interesting sharp decrease in Δ_{14} from CuCl, CuBr, to CuI. This is accurately accounted for by an increasing cancellation between $\Delta_{14}(C)$ and $\Delta_{14}(E_h)$ along this series, resulting from the increasing anion radius (i.e., increasing ρ). It is interesting to note that the signs of both the ionic and size contributions [$\Delta(C)$ and $\Delta(E_h)$] are opposite to the usual situation (e.g., ZnO) for which the partial cancellation is produced by a positive ionicity term $\Delta(C) > 0$ (no d electrons) and a negative size contribution $\Delta(E_h) < 0$ (i.e., $\rho > 0$).

D. Low-Ionicity First-Row Compounds

The compounds BP, BAs, and SiC all have first-row atoms together with low ionicities. The ionicities of BP and BAs are exceptionally small, $f_i = 0.058$, 0.026, respectively, and result from a near equality between Z_α/Z_β and r_α/r_β (i.e., $Z_\alpha/r_\alpha \simeq Z_\beta/r_\beta$). Therefore, the precise values for r_α and r_β are more important for these crystals than is usually the case, e.g., if $r_\alpha = r_\beta$ in SiC then $f_i = 0$; thus since $\Delta Z = 0$, the entire SiC ionicity is due to the difference in radii. As discussed in I this sensitivity to radii means that Eq. (19) must be evaluated using the actual radii r_α and not the average radius r_0; Eqs. (58) and (51) must therefore be modified. Further, in view of this radii sensitivity for these few crystals it would seem reasonable to also modify Eqs. (59) and (52).[57]

The only crystal of this set which has been measured is SiC.[57] The fact that the Δ calculated directly from Eqs. (55)–(59) is approximately a factor of 2 too large also suggests the need for a modified treatment. Because these few crystals require special treatment we do not discuss them here.

VII. REVIEW OF $A^N B^{8-N}$ COMPOUNDS

In order to exhibit more clearly the good agreement between theory and experiment, we plot the results of Tables III, IV, and VI in Fig. 4. The straight line is theory, and its satisfactory account of both the positive and negative nonlinear coefficients is evident. It is achieved without fitting any parameters to the nonlinear susceptibilities. The good agreement is also indicated by the small value for the deviation σ defined as

$$\sigma^2 = \frac{1}{n}\sum_1^n \left(\frac{d(\mathrm{calc}) - d(\mathrm{expt})}{d(\mathrm{calc})}\right)^2. \tag{79}$$

This deviation is only $\sigma = 19\%$ for the crystals in Fig. 4.[58] As previously mentioned, the interesting case of BeO, for which $\Delta_{33} \simeq 0$, is due to the near cancellation between $\Delta(C)$ and $\Delta(E_h)$. This leads to a nearly centrosymmetric bond even though both ρ and f_i are large. It is noteworthy that with one simple theory we have been able to treat crystals having a rather wide variation in their physical properties, i.e., III-V, II-VI, and I-VII crystals, both high and low ionicities, large and small band gaps (a factor of ~40 for the minimum gap between InSb and BeO), bonds composed of atoms having either the same or widely different radii, positive or negative nonlinearities, and noble-metal d-electron contributions to d_{ijk}. At present, the bond-

TABLE VI. Comparison between theoretical Δ_{14}^{calc} and experimental Δ_{14}^{expt} nonlinearities. The numbers in parentheses next to the Δ values are for $|d_{14}^{calc}|$ and $|d_{14}^{expt}|$ in units of 10^{-9} esu. The experimental numbers are an average of the similar values obtained at 0.946, 1.06, and 1.32 μ. Conversion from relative to absolute nonlinearities was done using Ref. 77.

Crystal	ρ	$F^{\mu}\Delta_{ijk}^{\mu}(C)$ (10^{-6} esu)	$F^{\mu}\Delta_{ijk}^{\mu}(E_h)$ (10^{-6} esu)	Δ_{ijk}^{calc} (10^{-6} esu)	Δ_{ijk}^{expt} (10^{-6} esu)
I-VII					
CuCl (14)	−0.20	−2.94	+1.75	−1.19 (13.0)	−1.33[a,b] (14.5)
CuBr (14)	−0.24	−3.17	+2.32	−0.85 (15.7)	−0.82[b] (15.1)
CuI (14)	−0.28	−3.25	+3.07	−0.18 (7)	−0.27[b] (10.2)
AgI (14)	−0.20	−3.94	+2.77	−1.17	

[a]R. C. Miller, S. C. Abrahams, R. L. Barns, J. L. Bernstein, W. A. Nordland, and E. H. Turner, Solid State Commun. 9, 1463 (1971).

[b]R. C. Miller, W. A. Nordland, S. C. Abrahams, and C. Schwab, Phys. Rev. (to be published).

charge model is the only theory which gives a good account of this wide range of crystals. This is especially true for the more complex crystals to be discussed shortly.

It is instructive to compare our model with other calculations for d_{ijk}. This is done in Table VII using only the simple $A^{III}B^{V}$'s since the other calculations are most successful for these crystals. A useful measure of the theoretical accuracy is the deviation σ [Eq. (79)] which is given along with the ratio σ/σ_L of these deviations to that of our bond-charge model σ_L. As Table VII shows, the bond-charge model is significantly more accurate, even for these simple $A^{III}B^{V}$ compounds.

Before turning to more complex compounds it may be worthwhile to make a few general comments concerning the successes of the bond-charge model. Since the model uses the measured macroscopic susceptibility χ as an input parameter, most of the local-field effects are automatically included. This is important since d_{ijk} is related to the *cube* of the local-field factor f, and therefore inaccuracies in the determination of f are a larger potential source of error in d_{ijk} than in χ. Also our theory for the *nonlinear* susceptibility is approximately self-consistent since unknown parameters (e.g., b, q, C, E_g, f_i, etc.) are determined from the *linear* susceptibility. For example, we determine the ionicity dielectrically, which seems more appropriate for the evaluation of d_{ijk} than does say Pauling's ionicity scale[56] which is determined from heats of formation.

VIII. SiO_2, GeO_2

Having satisfactorily explained the nonlinear optical susceptibility of the eight-electron $A^N B^{8-N}$

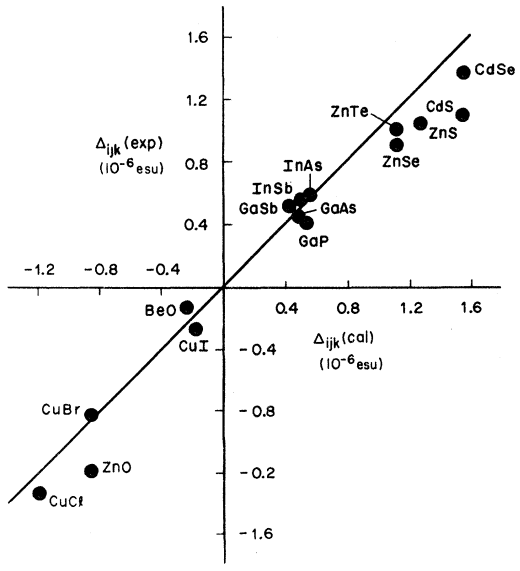

FIG. 4. Plot of experimental-vs-theoretical Miller's Δ's for the $A^N B^{8-N}$ compounds. The agreement between theory and experiment is excellent as demonstrated by the small standard deviation of only 19%.

TABLE VII. Comparison between experiment and various theoretical calculations of d_{14} (in 10^{-9} esu) for the simple $A^{III}B^{V}$ semiconductors. The standard deviation σ between theory and experiment is given as is the σ ratio between our calculation (σ_L) and the others.

$A^{III}B^{V}$	FD[a]	PV[b]	K[c]	A[d]	B[e]	M[f]	L[g]	Expt.[h]
GaP	350	425	375	120	179	100	130	99
GaAs	475	610	540	190	334	195	230	215
GaSb	400	1180	965	350	450	520	520	650
InAs	1030	785	855	320	600	305	410	430
InSb	1630	1410	1430	550	1140	660	790	870
σ	59%	56%	53%	50%	36%	26%	16%	
Ratio (σ/σ_L)	3.7	3.5	3.3	3.1	2.3	1.6	1.0	

[a]Chr. Flytzanis and J. Ducuing, Phys. Rev. 178, 1218 (1969).

[b]J. C. Phillips and J. A. Van Vechten, Phys. Rev. 183, 709 (1969).

[c]D. A. Kleinman, Phys. Rev. B 2, 3139 (1970).

[d]D. E. Aspnes, Phys. Rev. B 6, 4648 (1972).

[e]M. I. Bell, thesis (Brown University, 1972) (unpublished).

[f]R. C. Miller, Appl. Phys. Letters 5, 17 (1964). That is, the values in this column were obtained by using Miller's rule and scaling Δ to fit GaP.

[g]This paper.

[h]See references in Table III.

semiconductors, we turn to consider some more complex structures. We begin with the 16-electron quartz AB_2 structure (e.g., SiO_2 and GeO_2). All the linear-bond parameters necessary for the evaluation of Eqs. (55)–(59) are given in I with the exception of ρ, which we obtain directly from the covalent radii tables[43] [and Eq. (40)]. The geometrical factors[59] $G_{11} \equiv G_{111} = +0.0806$ (for right-handed[60] quartz) and $G_{14} \equiv G_{123} = 0$ are easily evaluated from Eq. (49). The result for right-handed quartz $SiO_2(r)$ shown in Table VIII is in good agreement with experiment both in magnitude and sign. Kleinman symmetry[47] is well satisfied by the experimental measurements since $\Delta_{14}^{\text{expt}} < 0.02 \times 10^{-6}$, in adequate agreement with the calculated value $\Delta_{14} = 0$. We note that the negative sign of $\Delta_{11}(SiO_2)$ is due to the dominance of the radii term $\Delta_{11}(E_h)$ just as in BeO and ZnO. This experimental agreement is achieved using exactly the same expressions [e.g., Eqs. (3), (55)–(59), etc.] as for the previously considered $A^N B^{8-N}$ semiconductors. Of course the bond parameters appropriate to SiO_2 are used, e.g., $n_v = 4$ in Eq. (9) as previously discussed, $n/m = 2$ in Eq. (58), etc.

IX. $NaClO_3$, $NaBrO_3$

Although $NaClO_3$ and $NaBrO_3$ are isomorphic, they have quite different nonlinear optical properties. The magnitude of Δ_{14} for $NaClO_3$ is ~5 times larger than that for $NaBrO_3$ and of opposite sign. This unusual behavior was first pointed out by Simon and Bloembergen[60] several years ago, but has not yet been fully explained. However, these nonlinearities can now be quantitatively understood by substituting the appropriate values into Eqs. (9), (55)–(59), etc. Some of the necessary parameters are $G_{14}(NaClO_3) = +0.1386$ and $G_{14}(NaBrO_3) = +0.1232$ (for the A configuration)[59]; $n_v = \frac{26}{3}$; $Z_\alpha + (n/m)Z_\beta = 7 + 3(6) = 25$; $r_\alpha(Cl) = 0.991$ Å, $r_\alpha(Br) = 1.077$ Å, $r_\beta(O) = 0.604$ Å (from I); and $N_e = (4)(26)/a^3\Phi$, where there are four molecules per cubic cell (volume a^3) and the fraction Φ of the unit cell occupied by the covalently bonded ClO_3 and BrO_3 units is also given in I as are all other necessary parameters. As shown in Table IX, our simple bond-charge theory nicely explains both the large difference in the nonlinearities as well as the sign reversal in these two crystals. Basically the explanation of this unusual behavior is that in $NaBrO_3$ the two acentricity contributions nearly cancel, leaving a small positive total nonlinearity $\Delta_{14}(C) > \Delta_{14}(E_h)$, whereas the lower ionicity in $NaClO_3$ causes $\Delta_{14}(C)$ to decrease and $\Delta_{14}(E_h)$ to increase. This changes the net sign and severely reduces the degree of cancellation.

X. MULTIBOND COMPOUNDS–$A^I B^{III} C_2^{VI}$ NOT CONTAINING NOBLE METALS, e.g., $LiGaO_2$

The method of decomposing multibond crystals such as $LiGaO_2$ ($ZnGeP_2$, $AgGaS_2$, etc.) into their constituent bond properties is described in some detail in I, and the necessary bond parameters are listed there. The $LiGaO_2$ geometrical factors[61] are $G_{33} = +0.222$ for both bonds, $F^\mu = \frac{1}{2}$, and the ρ^μ values are obtained from the VP covalent-radii tables. The contributions of the individual bonds are exhibited in Table X as well as the total calculated nonlinear coefficient. The cancellation between $\Delta_{33}(C)$ and $\Delta_{33}(E_h)$ for both the Li-O and Ga-O bonds is particularly pronounced especially for the Li-O bond in which the cancellation is practically complete. These near cancellations lead to a rather small total nonlinearity in agreement with experiment. It is obviously desirable to avoid such near cancellations when searching for new nonlinear optical materials having large coefficients. This small total nonlinearity is similar to the situation occurring in BeO. As discussed previously, the nonlinearity along the polar axis $\Delta_{33}(BeO)$ can be accurately obtained from the expected geometrical factor G_{33}, whereas the other coefficients Δ_{31} and Δ_{15} cannot, because of their small geometrical factors coupled with the strong cancellation between $\Delta(C)$ and $\Delta(E_h)$. An analogous situation exists for $LiGaO_2$, where Δ_{33} can be accurately calculated, whereas the other coefficients are more difficult.

XI. MULTIBOND COMPOUNDS–$A^{II} B^{IV} C_2^{V}$, e.g., $CdGeAs_2$, $ZnGeP_2$, etc.

As all the necessary parameters for the calculation are discussed and tabulated in I (except for $\rho = 0$ and $G_{36} = +0.193$)[59] we can immediately obtain the Miller Δ_{36} for these compounds (in Table XI).

TABLE VIII. Comparison between theoretical $\Delta_{11}^{\text{calc}}$ and experimental $\Delta_{11}^{\text{expt}}$ nonlinearities for right-handed enantiomorphs (r). The numbers in parentheses next to the Δ values are for $|d_{11}^{\text{calc}}|$ and $|d_{11}^{\text{expt}}|$ in units of 10^{-9} esu, at 1.06 μ.

Crystal	ρ	$F^\mu \Delta_{ijk}^\mu(C)$ (10^{-6} esu)	$F^\mu \Delta_{ijk}^\mu(E_h)$ (10^{-6} esu)	$\Delta_{ijk}^{\text{calc}}$ (10^{-6} esu)	$\Delta_{ijk}^{\text{expt}}$ (10^{-6} esu)
$SiO_2(r)$ (11)	+0.272	+0.46	−1.10	−0.64 (0.81)	−0.63[a,b] (0.80)
$GeO_2(r)$ (11)	+0.287	+0.35	−1.12	−0.77	

[a]B. F. Levine and C. G. Bethea, Appl. Phys. Letters 20, 272 (1972).

[b]R. C. Miller and W. A. Nordland, Phys. Rev. B2, 4896 (1970).

TABLE IX. Comparison between theoretical Δ_{14}^{calc} and experimental Δ_{14}^{expt} Miller's Δ's for the A configuration of $NaClO_3$ and $NaBrO_3$. The numbers in parentheses next to the Δ values are for $|d_{14}^{calc}|$ and $|d_{14}^{expt}|$ in units of 10^{-9} esu, at 0.6943 μ. Conversion from relative to absolute nonlinearities was done using Ref. 77.

Crystal	ρ	$F^{\mu}\Delta_{ijk}^{\mu}(C)$ (10^{-6} esu)	$F^{\mu}\Delta_{ijk}^{\mu}(E_h)$ (10^{-6} esu)	Δ_{ijk}^{calc} (10^{-6} esu)	Δ_{ijk}^{expt} (10^{-6} esu)
$NaClO_3$ (14)	+0.243	+0.65	−1.67	−1.02 (1.08)	−1.0[a,b] (1.06)
$NaBrO_3$ (14)	+0.281	+0.88	−0.73	+0.15 (0.31)	+0.21[a,b] (0.43)

[a]H. J. Simon and N. Bloembergen, Phys. Rev. 171, 1104 (1968).

[b]R. C. Miller and W. A. Nordland, Phys. Rev. B 2, 4896 (1970).

For the available experimental values the agreement with our theory is quite good. It is worth noting that we have calculated these crystals using essentially no experimental input data on these $A^{II}B^{IV}C_2^{V}$ compounds. All the necessary parameters are obtained in I by extrapolation of AB crystals.

XII. MULTIBOND COMPOUNDS–$A^{III}B^{V}C_4^{VI}$, e.g., $AlPO_4$, $GaPO_4$

The results of calculating Δ_{11} for $AlPO_4$ and $GaPO_4$ using the known[1] linear properties and $G_{11} = +0.0806$[59] are listed in Table XII. The results are in good agreement with the measured value for $AlPO_4$. We will later need the individual bond nonlinearity Δ_{β}^{μ} [see Eq. (56)] of the P-O bond and for convenience it is

$$\Delta_{\beta}^{\mu}(\text{P-O}) = -1.24\times10^{-28} \text{ esu} . \tag{80}$$

XIII. MULTIBOND COMPOUNDS–$A^{I}B^{III}C_2^{VI}$, e.g., $AgGaS_2$, $CuInS_2$, etc.

Because of the loosely bound d electrons and strong p-d hybridization[62] in $A^{I}B^{III}C_2^{VI}$ compounds, we treat their noble-metal d electrons in an analogous manner to those in the noble-metal halides previously discussed. Most of the necessary parameters for these compounds are given in II. For the noble-metal-bond core radius we use exactly the same relations [i.e., Eqs. (66) and (71)] as were used for the noble-metal halides [the non-noble-metal bonds are treated as usual, i.e., Eq. (27)]. The bond charge for these noble-metal bonds is taken from Eq. (72), i.e., $n_v = \frac{7}{4}$, which may be compared with $n_v = 2$ for the noble-metal halides. Finally the covalent radii and ρ are obtained in a manner analogous to that used for the noble-metal halides. That is, the S or Se atom is simply obtained from the average of the covalent[43] and ionic radii,[56]

$$\begin{aligned} r_S &= [(1.127)(1.84)]^{1/2} = 1.44 \text{ Å} , \\ r_{Se} &= [(1.225)(1.98)]^{1/2} = 1.56 \text{ Å} , \end{aligned} \tag{81}$$

and the noble-metal (NM) radius is obtained from the nearest-neighbor distance, i.e.,

$$r_{NM} = d - r_{S,Se} . \tag{82}$$

The noble-metal radii obtained in this way are within a few percent of those previously obtained in the noble-metal halides. This is especially notewothy in view of the different crystal structures and different anion valencies involved. The resulting ρ's are listed in Table XIII.

The experimental agreement shown in Table XIII is good and, in particular, nicely explains the various trends in the nonlinearity, such as $\Delta(AgGaSe_2) > \Delta(AgGaS_2)$, $\Delta(CuGaSe_2) > \Delta(CuGaS_2)$; i.e., the selenides are larger than the corresponding sulfides, and $\Delta(AgGaSe_2) > \Delta(CuGaSe_2)$, $\Delta(AgGaS_2) > \Delta(CuGaS_2)$; i.e., the silver compounds have a larger Miller Δ than the corresponding copper ones. The theory further explains why one of the indium compounds, $AgInSe_2$, has a large Δ

TABLE X. Comparison between theoretical Δ_{33}^{calc} and experimental Δ_{33}^{expt} nonlinearities. The contributions of the Li-O and Ga-O bonds to the total nonlinearity are also shown. The numbers in parentheses next to the Δ values are for $|d_{33}^{calc}|$ and $|d_{33}^{expt}|$ in units of 10^{-9} esu, at 1.06 μ. Conversion from relative to absolute nonlinearities was done using Ref. 77.

Bond-crystal	ρ	$F^{\mu}\Delta_{ijk}^{\mu}(C)$ (10^{-6} esu)	$F^{\mu}\Delta_{ijk}^{\mu}(E_h)$ (10^{-6} esu)	Δ_{ijk}^{calc} (10^{-6} esu)	Δ_{ijk}^{expt} (10^{-6} esu)
		$LiGaO_2$			
Li-O (33)	+0.266	+0.16	−0.16	0.00	
Ga-O (33)	+0.287	+2.08	−2.46	−0.38	
$LiGaO_2$ (33)				−0.38 (1.70)	−0.37[a,b] (1.66)

[a]R. C. Miller, W. A. Nordland, E. D. Kolb, and W. L. Bond, J. Appl. Phys. 41, 3008 (1970); R. C. Miller (private communication). (The last two columns in Table II of this reference should be increased by 10%.)

[b]R. C. Miller and W. A. Nordland, Phys. Rev. B 2, 4896 (1970).

while the other, $CuInS_2$, has an anomalously small value. This $CuInS_2$ example is interesting since it illustrates the nature of the various contributions (and their partial cancellations) to d_{ijk}; thus the Cu-S bond in $CuInS_2$ has comparable contributions from the negative electronegativity term $\Delta(C)$ produced by the d-electron contributions, and the positive radius $\Delta(E_h)$ term caused by $r_S > r_{Cu}$; this partial cancellation results in a small net negative nonlinearity for the Cu-S bond, i.e., $\Delta(\text{Cu-S}) < 0$. This is analogous to the situation in BeO, $LiGaO_2$, and CuI. What is different in $CuInS_2$ (and most of the other noble-metal chalcopyrites) is that this net negative $\Delta(\text{CuS})$ then partially cancels the larger positive bond nonlinearity of InS resulting in a small net nonlinearity for the whole $CuInS_2$ crystal.

TABLE XI. Comparison between theoretical Δ_{36}^{calc} and experimental Δ_{36}^{expt} nonlinearities. The contributions of each type of bond to the total nonlinearity is also shown. The numbers in parentheses next to the Δ values are for $|d_{36}|$ in units of 10^{-9} esu, at 10.6 μ. Conversion from relative to absolute nonlinearities was done using Ref. 77.

	$A^{II}B^{IV}C_2^V$			
Bond-crystal	$F^{\mu}\Delta_{ijk}^{\mu}$ (10^{-6} esu)	Δ_{ijk}^{calc} (10^{-6} esu)	Δ_{ijk}^{expt} (10^{-6} esu)	
Zn-P (36)	+0.13			
Si-P (36)	+0.41			
$ZnSiP_2$ (36)		+0.54		
Cd-P (36)	+0.20			
Si-P (36)	+0.48			
$CdSiP_2$ (36)		+0.68		
Zn-P (36)	+0.12			
Ge-P (36)	+0.55			
$ZnGeP_2$ (36)		+0.67 (220)	± 0.55[a]	(180)
Cd-P (36)	+0.16			
Ge-P (36)	+0.64			
$CdGeP_2$ (36)		+0.80 (290)	± 0.71[a]	(260)
Zn-P (36)	+0.11			
Sn-P (36)	+0.89			
$ZnSnP_2$ (36)		+1.00		
Cd-P (36)	+0.15			
Sn-P (36)	+0.96			
$CdSnP_2$ (36)		+1.11		
Zn-As (36)	+0.14			
Si-As (36)	+0.49			
$ZnSiAs_2$ (36)		+0.63 (250)	± 0.44[a]	(175)
Cd-As (36)	+0.22			
Si-As (36)	+0.55			
$CdSiAs_2$ (36)		+0.77		
Zn-As (36)	+0.10			
Ge-As (36)	+0.42			
$ZnGeAs_2$ (36)		+0.52		
Cd-As (36)	+0.15			
Ge-As (36)	+0.50			
$CdGeAs_2$ (36)		+0.65 (500)	± 0.73[a,b]	(560)
Zn-As (36)	+0.07			
Sn-As (36)	+0.32			
$ZnSnAs_2$ (36)		+0.39		
Cd-As (36)	+0.10			
Sn-As (36)	+0.39			
$CdSnAs_2$ (36)		+0.49		

[a]G. D. Boyd, E. Buehler, F. G. Stortz, and J. H. Wernick, IEEE J. Quantum Electron. QE-8, 419 (1972).
[b]R. L. Byer, H. Kildal, and R. S. Feigelson, Appl. Phys. Letters 19, 237 (1971).

XIV. MULTIBOND COMPOUNDS–KH_2PO_4

The crystal KH_2PO_4 (KDP) is interesting from several viewpoints. It is the prototype of several similar compounds such as $(NH_3)H_2PO_4$, CsH_2PO_4, RbH_2PO_4, KH_2AsO_4, CsH_2AsO_4, RbH_2AsO_4, and the deuterated form of the above compounds, e.g., KD_2PO_4. In addition KDP has a paraelectric-ferroelectric phase transition which has been the object of extensive investigations.[83] The rather complex unit cell of KDP is also of interest as it enables us to test further our noninteracting-bond assumption.

For simplicity we will calculate the nonlinearity in the paraelectric phase. The H-O bonds do not contribute to the nonlinear coefficient in this phase since they are disordered and therefore average to zero. (In the ferroelectric state these H-O bonds become ordered and then do contribute significantly to the nonlinear optical susceptibility.[64]) Further, since the K^+ ion would only be expected to contribute a negligible amount (this may be slightly less true for say Rb^+ in RDP), almost all of the nonlinearity resides in the P-O bonds. Although the H-O bonds do not contribute to the nonlinear susceptibility (they are centrosymmetric on the average), they do of course contribute to the linear susceptibility; therefore, since their linear susceptibility is expected to be significant, we cannot simply evaluate Δ_{ijk} for the P-O bonds by using the total net measured susceptibility of KDP, i.e., $\chi^{\mu}(\text{P-O}) \neq \chi(\text{KDP})$.

In order to avoid this problem of decomposing $\chi(\text{KDP})$ into its constituent bond susceptibilities we can try the simple assumption that $\Delta_{\beta}(\text{P-O})$ in KH_2PO_4 (in which the P is tetrahedrally surrounded by O) has the same value as for the P-O bond in $AlPO_4$ [Eq. (80)], where the P is also tetrahedral, i.e., in KDP,

$$\Delta_{\beta}(\text{P-O}) \simeq -1.24\times10^{-28} \text{ esu} . \quad (83)$$

It is important to note that this similarity assumption can *only* work for bonds that are in comparable host environments. For example, the tetrahedrally coordinated Al atom for the Al-O bond in $AlPO_4$ is *not* like the octahedral Al-O bond in Al_2O_3 (their ionicities, for example, are $f_i = 0.65$ and 0.80, re-

TABLE XII. Comparison between theoretical Δ_{11}^{calc} and experimental Δ_{11}^{expt} Miller's Δ's for right-handed (r) enantiomorphs. The numbers in parentheses are for $|d_{11}|$ in units of 10^{-9} esu, at 1.06 μ. Conversion from relative to absolute nonlinearities was done using Ref. 77.

			$A^{III}B^{V}C_4^{VI}$			
Bond-crystal		ρ	$F^{\mu}\Delta_{ijk}^{\mu}(C)$ (10^{-6} esu)	$F^{\mu}\Delta_{ijk}^{\mu}(E_h)$ (10^{-6} esu)	Δ_{ijk}^{calc} (10^{-6} esu)	Δ_{ijk}^{expt} (10^{-6} esu)
Al-O	(11)	+0.293	+0.13	−0.30	−0.17	
P-O	(11)	+0.249	+0.33	−0.85	−0.52	
$AlPO_4(r)$	(11)				−0.69 (0.78)	± 0.80[a] (0.90)
Ga-O	(11)	+0.287	+0.15	−0.44	−0.29	
P-O	(11)	+0.249	+0.19	−0.51	−0.32	
$GaPO_4(r)$	(11)				−0.61	

[a]R. C. Miller, Appl. Phys. Letters 5, 17 (1964), and private communication.

spectively).

Using the approximate Eq. (83) we can calculate Δ_{36} for KDP from

$$\Delta_{36}(\text{KDP}) = G_{36}N_b\Delta_\beta(\text{P-O}) , \tag{84}$$

where the geometrical factor for the P-O bonds in KDP is $G_{36} = -0.163$ [59] and the number of P-O bonds per/cm^3 in KDP [59] is $N_b = 4.134\times10^{22}$. The comparison with experiment[65] given below can be seen to be good both in magnitude and sign:

$$\begin{aligned}\Delta_{36}(\text{calc}) &= +0.84\times10^{-6}\ \text{esu} ,\\ \Delta_{36}(\text{expt}) &= +1.18\times10^{-6}\ \text{esu} .\end{aligned} \tag{85}$$

This agreement shows that one can indeed use the bond nonlinearity determined from one crystal in a different compound as long as the two crystals are sufficiently similar. This can be a rather useful procedure[27] and we employ it further in the following section.

XV. FERROELECTRICS, e.g., $LiNbO_3$, $LiTaO_3$, $Ba_2NaNb_5O_{15}$

The nonlinear optical properties of oxygen-octahedra ferroelectrics such as $LiNbO_3$ and $Ba_2NaNb_5O_{15}$ have been studied extensively[66] because of their very favorable properties; e.g., they are transparent in the visible, they can be noncritically phase matched for second-harmonic

TABLE XIII. Comparison between calculated and experimental nonlinearities. The contributions of each type of bond to the total nonlinearity is also shown. The numbers in parentheses next to the Δ_{36} are for $|d_{36}|$ in units of 10^{-9} esu at 10.6 μ. Conversion from relative to absolute nonlinearities was done using Ref. 77.

			$A^{I}B^{III}C_2^{VI}$			
Bond-crystal		ρ	$F^{\mu}\Delta_{ijk}^{\mu}(C)$ (10^{-6} esu)	$F^{\mu}\Delta_{ijk}^{\mu}(E_h)$ (10^{-6} esu)	Δ_{ijk}^{calc} (10^{-6} esu)	Δ_{ijk}^{expt} (10^{-6} esu)
Cu-S	(36)	−0.21	−0.86	+0.67	−0.19	
Ga-S	(36)	0	+0.67	0	+0.67	
$CuGaS_2$	(36)				+0.48 (30)	± 0.37[a] (23)
Cu-S	(36)	−0.19	−1.43	+1.07	−0.36	
In-S	(36)	0	+0.65	0	+0.65	
$CuInS_2$	(36)				+0.29 (23)	± 0.21[a] (17)
Cu-Se	(36)	−0.26	−1.04	+1.18	+0.14	
Ga-Se	(36)	0	+0.60	0	+0.60	
$CuGaSe_2$	(36)				+0.74 (94)	± 0.56[b] (71)
Ag-S	(36)	−0.13	−0.77	+0.40	−0.37	
Ga-S	(36)	0	+0.96	0	+0.96	
$AgGaS_2$	(36)				+0.59 (27)	± 0.63[a] (29)
Ag-Se	(36)	−0.18	−0.75	+0.60	−0.15	
Ga-Se	(36)	0	+0.96	0	+0.96	
$AgGaSe_2$	(36)				+0.81 (72)	± 0.86[b] (79)
Ag-Se	(36)	−0.17	−0.87	+0.65	−0.22	
In-Se	(36)	0	+1.09	0	+1.09	
$AgInSe_2$	(36)				+0.87 (91)	± 0.86[b] (90)

[a]G. D. Boyd, H. Kasper, and J. H. McFee, IEEE J. Quantum Electron. QE-7, 563 (1971).

[b]G. D. Boyd, H. M. Kasper, J. H. McFee, and F. G. Storz, IEEE J. Quantum Electron. QE-8, 900 (1972).

generation, and the indices of refraction are significantly temperature dependent making noncritical phase matching at various wavelengths and also temperature-tuned parametric oscillators possible.[66] These crystals have large refractive indices $n > 2$, and $Ba_2NaNb_5O_{15}$ has the largest phase-matchable nonlinear coefficient in the *visible* region of any presently known material.[67]

One of the most successful approaches for understanding the origin of the nonlinear susceptibility in these materials is the geometrical analysis of Jeggo and Boyd.[27] These authors show that the full tensor character of d_{ijk} can be accurately accounted for in terms of experimentally determined bond nonlinearities β [i.e., by substituting these β's into a relation like Eq. (47)]. The different tensor elements of d_{ijk} arise directly from the geometry of the bonds [i.e., Eq. (49)]. From the viewpoint of our bond-charge theory the success of the Jeggo and Boyd bond approach can be readily understood. The important problem which now remains is the theoretical calculation of Jeggo and Boyd's empirically determined bond parameters β and Δ_β, for each of the inequivalent bonds. Only the transition-metal–oxygen bonds are expected to make important contributions to d_{ijk}[27] since the other bonds (e.g., Li-O in $LiNbO_3$) are significantly more ionic and less polarizable. A similar situation can be seen in, say, $LiGaO_2$ (Table X), where $\Delta(C)$ for the Li-O bond is more than an order of magnitude smaller than for the Ga-O bond.

Most of the parameters necessary for the evaluation of Eqs. (55)–(59), (72), etc., are given in II. As previously discussed for the noble-metal compounds, the Z_α in Eq. (58) should be replaced by Z_α^*, the effective core charge including the transition-metal d electrons. Owing to the intermediate ionicity $f_i \simeq 0.83$ for $LiNbO_3$ and $LiTaO_3$, we evaluate ρ in a manner analogous to that used for the noble-metal compounds. That is, we obtain the O radius[43,56] from Eq. (73),

$$r_O = [(0.678)(1.40)]^{1/2} = 0.97 \text{ Å} , \tag{86}$$

and r_{Nb} (or r_{Ta}) from the bond length. Since $d = 2.00$ Å for $LiNbO_3$ (or $d = 1.98$ Å for $LiTaO_3$), we see that the transition-metal and oxygen radii are closely equal and

$$\rho \simeq 0 . \tag{87}$$

Thus we only need to consider the ionic contribution to Δ_{ijk}, i.e., Eq. (58). A straightforward evaluation of the individual bond nonlinearity yields the values listed in Table XIV. The comparison between the experimentally determined values of Jeggo and Boyd[27] and our theoretical values shows good agreement in both magnitude and sign.

In order to calculate the full tensor Δ_{ijk}, we must know not only the average values of the nonlinearity β or Δ_β (which we have just evaluated) but also its *dependence on the bond length.* It is important to note here that we never required this information before, since for all previous compounds we could directly obtain Δ_{ijk} from Δ_β using Eq. (55). However, this is no longer true since the inversion symmetry at the Nb (Ta) site is broken only by small displacements of the Nb (or Ta) and O atoms.[68] That is, Δ_{ijk} would equal zero if all the bond lengths were identical. Moreover, even with the proper inclusion of the different bond lengths, the result $\Delta_{31} \simeq 0$ in $LiNbO_3$ and $LiTaO_3$ would still be obtained unless β and Δ_β vary with d. The dependence on bond length which was empirically chosen by Jeggo and Boyd[27] (JB) to give the best fit to experiment for the Nb-O bonds was

$$\beta_{JB} \propto 39.7 + 0.130 d^7 . \tag{88}$$

To compare Eq. (88) with our theory we begin with our expression for β, namely, Eqs. (48) and (51),

$$\beta \propto e^{-k_s r_0} \chi_b^2 C / E_g^2 d^2 , \tag{89}$$

where we have only included the quantities which depend on the bond length d (e.g., $N_b = \text{const}$). It is convenient to write the dependence of β on d as

$$\beta = \beta_0 (d/d_0)^\sigma , \tag{90}$$

where β_0 is the average bond nonlinearity (which we have already calculated in Table XIV), d_0 the average bond length ($= 2.00$ Å in $LiNbO_3$), and σ is the power dependence $\beta \propto d^\sigma$. Thus,

$$\sigma = \frac{d}{\beta} \frac{\partial \beta}{\partial d} \tag{91}$$

and by substituting Eq. (89) into Eq. (91) σ can be evaluated theoretically. We see that we must now differentiate our relation for β, which was in turn obtained by differentiating the expression for the linear susceptibility [see Eq. (35)]; i.e., the determination of σ involves something like a second derivative. Needless to say, this is a severe test of our simple bond-charge model, and a correct prediction of the functional dependence of β on d would be a somewhat unexpected bonus. Proceed-

TABLE XIV. Comparison between the theoretical Δ_β(calc) and experimental Δ_β(expt) Miller's Δ's for a *single* bond. The numbers in parentheses are for the nonlinear susceptibility for a *single* bond β in units of 10^{-30} esu at 1.06 μ. Conversion from relative to absolute nonlinearities was done using Ref. 77.

Crystal	Δ_β(calc) (10^{-28} esu)	Δ_β(expt) (10^{-28} esu)
$LiNbO_3$(Nb-O)	+2.0 (6.3)	+1.9[a] (6.0)
$LiTaO_3$(Ta-O)	+1.7 (3.9)	+1.9[a] (4.3)

[a]C. R. Jeggo and G. D. Boyd, J. Appl. Phys. 41, 2741 (1970).

ing as indicated one finds

$$\sigma = -\tfrac{1}{2}k_s r_0 + 2\,\frac{d}{\chi_b}\,\frac{\partial \chi_b}{\partial d} + \frac{d}{C}\,\frac{\partial C}{\partial d} - \frac{d}{E_g^2}\,\frac{\partial E_g^2}{\partial d} - 2\ . \tag{92}$$

Then, using $\chi_b \propto \Omega^2/E_g^2$ with $\Omega^2 \propto d^{-3}$ and Eqs. (16)–(19), it is readily shown that

$$\sigma = [6s - k_s r_0 - 9] - [6(s-1) - 3k_s r_0] f_i\ , \tag{93}$$

where $s = 2.48$ from Eq. (18). Substituting the known parameters from II (i.e., $k_s r_0 = 2.363$, $f_i = 0.825$ for $LiNbO_3$), one finds

$$\sigma(LiNbO_3) = 2.0\ ,$$

i.e.,

$$\beta = \beta_0 (d/d_0)^2 \propto d^2\ . \tag{94}$$

For later reference we note that Eq. (93) also predicts $\beta \propto d^2$ for the Ta-O bond in $LiTaO_3$. This Eq. (94) is to be compared with Jeggo and Boyd's experimental determination, Eq. (88). Although Eq. (88) may look like a d^7 dependence while Eq. (94) is only a d^2 dependence, this is not the case. Substituting Eq. (88) into Eq. (91) shows that in fact

$$\sigma_{JB} = \frac{7(0.13)d^7}{39.7 + 0.13 d^7} = 2.1\ , \tag{95}$$

in very good agreement with our calculated value in Eq. (94) of $\sigma = 2.0$.

We are now in a position to calculate the full tensor d_{ijk} coefficient for these transition-metal ferroelectrics. For example, the relations for $LiNbO_3$ are[27]

$$\begin{aligned} d_{31} &= N(1.104\beta_1 - 1.106\beta_2)\ , \\ d_{22} &= N(0.396\beta_1 - 0.195\beta_2)\ , \\ d_{33} &= N(0.643\beta_1 - 1.796\beta_2)\ , \end{aligned} \tag{96}$$

where β_1 and β_2 refer to the short and long bonds, respectively (i.e., $d_1 = 1.89$ Å and $d_2 = 2.11$ Å), and N is the number of rhombohedral unit cells per/cm^3 (i.e., $N = 1/V$, where V is the rhombohedral unit-cell volume). The application of Eq. (94) for the dependence of β on d then yields

$$\begin{aligned} d_{31} &= -0.245 N\beta_0\ , \\ d_{22} &= +0.137 N\beta_0\ , \\ d_{33} &= -1.425 N\beta_0 \end{aligned} \tag{97}$$

or using the Δ_{ijk} formulation

$$\begin{aligned} \Delta_{31} &= -0.245 N\Delta_\beta\ , \\ \Delta_{22} &= +0.137 N\Delta_\beta\ , \\ \Delta_{33} &= -1.425 N\Delta_\beta\ , \end{aligned} \tag{98}$$

where Δ_β has already been calculated for $LiNbO_3$ and is given in Table XIV ($\Delta_\beta^{calc} = 2.0\times10^{-28}$ esu). Thus using $N = 0.943\times10^{22}$ cm^{-3}, one finds

$$\begin{aligned} \Delta_{31}^{calc}(LiNbO_3) &= -0.46\times10^{-6}\ \text{esu}\ , \\ \Delta_{22}^{calc}(LiNbO_3) &= +0.26\times10^{-6}\ \text{esu}\ , \\ \Delta_{33}^{calc}(LiNbO_3) &= -2.7\times10^{-6}\ \text{esu}\ , \end{aligned} \tag{99}$$

which is in good agreement with experiment as demonstrated in Table XV.

The agreement between our theory and experiment for the more complex niobates is not quite as good as for $LiNbO_3$. Considering the many close cancellations between the contributions of the various Nb-O bonds, the possible small contributions from the non-transition-metal bonds, the severe test of our theory when predicting the functional dependence of β on bond length, and the fact that we have not used any adjustable parameters, we feel that the over-all experimental agreement is quite reasonable, adequately explaining both the magnitude and sign of the nonlinearity of these ferroelectrics.

Generally our results are not as good as those of Jeggo and Boyd[27] (although, for example, our results for the complex $Ba_2NaNb_5O_{15}$ are actually somewhat better). This is of course to be expected since JB have two adjustable parameters (β_1 and β_2 in $LiNbO_3$) for the Nb-O bond and two more for the Ta-O bond in $LiTaO_3$. Our worst discrepancy is

TABLE XV. Comparison between calculated and experimental nonlinearities. The numbers in parentheses are for $|d_{ijk}|$ in units of 10^{-9} esu at 1.06 μ. For Δ_{31} of $LiNbO_3$ the value given is for the stoichiometric growth mixture, which was interpolated from the measurements of Miller *et al.* (Ref. c). For the other coefficients in $LiNbO_3$, and also for $LiTaO_3$, the values used are the averages of the various measurements in Refs. c and d, since these coefficients do not vary strongly with composition. Conversion from relative to absolute nonlinearities was done using Ref. 77.

Crystal		Δ_{ijk}^{calc}	Δ_{ijk}^{expt}
$LiNbO_3$	Δ_{31}	−0.46 (15)	−0.40[a,b] (13)
	Δ_{22}	+0.26 (9.2)	+0.15[c,b] (5.2)
	Δ_{33}	−2.7 (73)	−2.7[c,b] (71)
$Ba_2NaNb_5O_{15}$	Δ_{31}	−0.56 (20)	−0.92[d,b] (32)
	Δ_{32}	−0.66 (23)	−0.90[d,b] (31)
	Δ_{33}	−1.2 (33)	−1.6[d,b] (44)
$LiTaO_3$	Δ_{31}	−0.29 (6.7)	−0.10[e,b] (2.4)
	Δ_{22}	+0.15 (3.8)	+0.19[e,b] (4.8)
	Δ_{33}	−1.6 (39)	−1.6[e,b] (39)

[a]B. F. Levine and C. G. Bethea, Appl. Phys. Letters 20, 272 (1972).

[b]R. C. Miller and W. A. Nordland, Phys. Rev. B 2, 4896 (1970).

[c]R. C. Miller, W. A. Nordland, and P. M. Bridenbaugh, J. Appl. Phys. 42, 4145 (1971).

[d]S. Singh, D. A. Draegert, and J. E. Geusic, Phys. Rev. B 2, 2709 (1970).

[e]R. C. Miller (private communication).

$\Delta_{31}(LiTaO_3)$ which is not too surprising since it is in fact exceedingly sensitive to the functional form $\beta \propto d^{\sigma}$ and indeed vanishes completely for $\sigma \simeq 0$. This Δ_{31} coefficient (in $LiNbO_3$) has been observed[69] to vary significantly with the ratio of Li to Nb, whereas the other coefficients Δ_{22} and Δ_{33} remained practically constant; part of our error may be due to this type of difference between the crystal used for the x-ray determination of the atomic coordinates and the crystal in which the Δ_{ijk} were measured. It is also possible that the small Δ_{31} has a non-negligible contribution from the Li-O bond. It is worth noting that we do correctly predict $\Delta_{31}(LiTaO_3) < \Delta_{31}(LiNbO_3)$, and that the magnitude and sign of the bond nonlinearity is accurately predicted for $LiTaO_3$, as can be seen from both Table XIV and the good experimental agreement for Δ_{22} and Δ_{33}.

Jerphagnon[30] has shown a direct linear relationship between the vector part of Δ_{ijk} defined as $\Delta_v \equiv \Delta_{31} + \Delta_{32} + \Delta_{33}$, and the spontaneous polarization P_s, namely,

$$\Delta_v = -0.7\times10^{-7} P_s \text{ esu} , \tag{100}$$

where P_s is in units of $\mu C/cm^2$. This relation generally works rather well for a large number of materials although there are several exceptions (which we will discuss later). Using our theory for Δ_{ijk}, we can derive this close relationship between Δ_v and P_s.

For the sake of definiteness consider the C_{3v} crystal structure resulting from a polarization P_s lying along the threefold cubic axis (e.g., $LiNbO_3$, $LiTaO_3$). It is not difficult to show that a displacement of the transition metal, Δz, from the exact center of the oxygen octahedron results in a change in the bond lengths from d_0 to $d_0(1 \pm \frac{1}{3}\epsilon)$, where $\epsilon \equiv \Delta z/z = \sqrt{3}\,\Delta z/d_0$. This results in a difference in the bond nonlinearities β between the long and short bonds of $\beta = \beta_0(1 \pm \frac{2}{3}\epsilon)$, where use has been made of Eq. (94). This change in bond length for the six bonds, i.e., one formula unit (f) thus produces a contribution to d_{ijk} of

$$d^f_{33} = d^f_{32} = d^f_{31} = -(4/3\sqrt{3})\beta\epsilon \tag{101}$$

or

$$\Delta^f_{33} = \Delta^f_{32} = \Delta^f_{31} = -(4/3\sqrt{3})\Delta_\beta\epsilon . \tag{102}$$

There is another contribution to d_{ijk} from the rotation of the bonds which is caused by the displacement Δz. This contribution exists even if β remains constant, and can be readily evaluated to be

$$\Delta^f_{33} = -(12/3\sqrt{3})\Delta_\beta\epsilon , \qquad \Delta^f_{31} = \Delta^f_{32} = 0 . \tag{103}$$

Combining these two contributions, Eqs. (102) and (103), results in

$$\Delta^f_v = \Delta^f_{31} + \Delta^f_{32} + \Delta^f_{33} = -(24/3\sqrt{3})\Delta_\beta\epsilon . \tag{104}$$

It may be worth observing that for the dependence $\beta \propto d^2$ which we have used, Eqs. (102) and (103) show that rotation and bond stretching effects make equal contributions to Δ_v. To obtain the total nonlinearity we can simply multiply the Δ_v per formula unit, Eq. (104), by the number of units/$cm^3 = 2/V$ (V is the rhombohedral cell volume). Thus

$$\Delta_v = -(8\Delta_\beta/V)\Delta z . \tag{105}$$

We can now relate Δz to the polarization using the relation of Abrahams, Kurtz, and Jamieson,[70] i.e.,

$$P_s = \xi\Delta z \ \mu C/cm^2 , \tag{106}$$

where Δz is in Å and $\xi = 258$. This yields

$$\Delta_v = -(8\Delta_\beta/V\xi)P_s . \tag{107}$$

Using the values $\xi = 258$, $V = 106\times10^{-24}$ cm^3, and $\Delta_\beta = 2.0\times10^{-28}$ (from Table XIV) shows

$$\Delta_v = -0.6\times10^{-7} P_s \text{ esu} , \tag{108}$$

which is in agreement with Jerphagnon's empirically determined proportionality constant of -0.7×10^{-7} in Eq. (100).

As noted by several workers,[71] Jerphagnon's relation works rather well for a wide range of compounds; there are, however, some exceptions,[30,71] e.g., triglycine sulfate, $Pb_5Ge_3O_{11}$, and $PbTiO_3$.[72] The reasons[71] for these exceptions are twofold. First, Eq. (106) may be inaccurate for a particular compound in which several kinds of ions contribute to P_s, and second, there may be several types of bonds contributing to Δ_{ijk} which may not be those which are producing the polarization. For example, a highly ionic bond may strongly effect the spontaneous polarization because of its large ionic charges, but contribute only weakly to Δ_{ijk} because of its small polarizability. Conversely, covalent bonds tend to have large polarizabilities and large β's but may make only a small contribution to P_s.

XVI. HIGHLY ANISOTROPIC BONDS—HgS, Se, Te

Owing to the unusual "one-dimensional" nature of HgS, Se, and Te (each atom is bonded to only two nearest neighbors in a spiral arrangement) these crystals are highly anisotropic[1] with the susceptibility parallel to the bond axis $\chi_\parallel$ being much larger than that perpendicular to it $\chi_\perp$. More specifically, this anisotropy ratio $\chi_\parallel/\chi_\perp$ varies from 3.23 to 14.8 to 38.3 in HgS, Se, and Te, respectively. All the necessary parameters for the evaluation of the bond nonlinearity β are tabulated in I (ρ is taken as zero). The only real difference in the evaluation of Eq. (58) for these highly anisotropic bonds is that $\chi_\parallel = N_b(\chi^\mu_b)_\parallel$ and $\epsilon_\parallel$ should be used to determine q and $(\chi^\mu_b)_\parallel$. The geometrical factor G_{11} for HgS is easily evaluated from Eq. (49) and is $G_{11}(HgS) = 0.027$.[59] We can now calcu-

late the nonlinear coefficient Δ from Eq. (58). However, it should be remembered that Δ is *defined* so that the χ used in the *denominator* is the average macroscopic susceptibilities (obtained from the indices of refraction). The agreement with experiment shown in Table XVI is good especially in view of the highly anisotropic nature of this compound. The absolute sign of Δ(HgS) is of course dependent on definitions of axes. Since we are not aware of any standard conventions in this crystal it is clearest to state the sign of the *bond* nonlinearity is positive, $\beta > 0$ (where the positive direction is from the Hg to the S).

Most of the comments made about HgS and its anisotropy also apply to Se and Te; the major difference is the geometrical factor. There are three inequivalent Se or Te bonds per unit cell.[59] One of the bonds is perpendicular to the x axis ($\alpha_x' = 0$) and thus does not contribute to G_{11} or d_{11}. The other two bonds have a direction cosine of

$$\alpha_x = \frac{\pm \frac{3}{2}ua}{[3u^2a^2 + (\frac{1}{3}c)^2]^{1/2}} , \tag{109}$$

where a and c are the lattice constants of the hexagonal unit cell and u is the positional parameter describing the location of the atoms inside the unit cell. The $\pm$ sign indicates that the absolute direction of the very small bond dipole is difficult to ascertain, since the ionicity is so tiny, e.g., $f_i(\mathrm{Te}) \simeq 0.05$. Thus, neglecting the *absolute* sign, we take the α_x's of the two contributing bonds to have the same sign (taking opposite signs would incorrectly lead to $G_{11} = d_{11} = 0$) which then results in the geometrical factors

$$\begin{aligned} G_{11} &= \tfrac{2}{3}(\alpha_x)^3 \\ &= 0.15 \text{ for Se} \\ &= 0.16 \text{ for Te} . \end{aligned} \tag{110}$$

The rest of the calculation of the nonlinear optical susceptibility proceeds as for HgS. The results shown in Table XVI are good, which is especially satisfying in view of the enormous anisotropy ratios $\chi_\parallel/\chi_\perp = 14.8$ and 38.3, large parallel dielectric constants $\epsilon_\parallel = 21$ and 78.3, and also the small ionicities $f_i = 0.05$.

TABLE XVI. Comparison between calculated and experimental nonlinearities. The numbers in parentheses are for $|d_{11}|$ in units of 10^{-9} esu at 10.6 μ. Conversion for relative to absolute nonlinearities was done using Ref. 77.

Crystal	$\Delta_{ijk}^{\mathrm{calc}}$ (10^{-6} esu)	$\Delta_{ijk}^{\mathrm{expt}}$ (10^{-6} esu)
HgS (11)	0.8 (80)	1.2[a] (120)
Se (11)	1.8 (190)	2.2[b] (230)
Te (11)	0.6 (3200)	0.3[c] (1600)

[a]G. D. Boyd, T. J. Bridges, and E. G. Burkhardt, IEEE J. Quantum Electron. QE-4, 515 (1968).
[b]G. W. Day, Appl. Phys. Letters 18, 347 (1971).
[c]B. F. Levine and C. G. Bethea, Appl. Phys. Letters 20, 272 (1971).

It is worth noting that our calculation explains the otherwise puzzling experimental observation that Δ_{11}(Se) and Δ_{11}(Te) have rather normal values; i.e., the nonlinearity is not anomalously small as would be expected from the monoatomic composition and consequent small ionicity for these crystals. On the contrary, Se has an anomalously *large* Δ. The reason for this is simply the huge anisotropy, i.e., the large susceptibility parallel to the bond axis $\chi_\parallel$ which greatly increases the nonlinear coefficient d_{ijk}. A true measure of the intrinsic Miller Δ for these materials is

$$\Delta_{ijk}(\mathrm{intrin.}) = d_{ijk}/(\chi_\parallel)^3 \tag{111}$$

and not Eq. (54), where the average susceptibility χ_{av} is used. Since, for example, in Te $\chi_\parallel/\chi_{\mathrm{av}} = 2.85$, the intrinsic Δ_{ijk} is reduced by a factor $(2.85)^3 = 23$ or

$$\Delta_{11}^{\mathrm{Te}}(\mathrm{intrin.}) = 0.3\times10^{-6}/23 \simeq 0.01\times10^{-6} \text{ esu} , \tag{112}$$

which is indeed almost two orders of magnitude smaller than usual.[18] For Se

$$\Delta_{11}^{\mathrm{Se}}(\mathrm{intrin.}) \simeq 0.1\times10^{-6} \text{ esu} , \tag{113}$$

which is roughly one order of magnitude smaller than usual.[18]

XVII. COMMENTS ON DESIRABLE BOND PARAMETERS

It may be useful to review here some of the favorable bond properties that can lead to a large nonlinear coefficient. From Eq. (47) we see that one important consideration is the geometrical factor G_{ijk}. Obviously a small G_{ijk} can reduce the usefulness of a large bond nonlinearity β as, for example, in $LiNbO_3$, where the factor[73] $G_{31} = 0.017$ is an order of magnitude smaller than that for zinc blende.

The tetrahedral zinc-blende structure is an example of a crystal with a large geometrical factor, $G_{36} = 1/3\sqrt{3} = 0.192$. Although its cubic symmetry does not allow birefringence for phase matching, the similar tetragonal chalcopyrite structure has the same geometrical factor and can be phase matched. It may be worth noting that G_{36} in zinc blende is a factor of $\sqrt{3}$ larger than the phase matchable component G_{31} of the similar hexagonal wurtzite structure.

Another important consideration in Eq. (47) is the number N_b of bonds per/cm^3. Clearly the zinc-blende and wurtzite crystals have the largest possible values since there is only one type of bond (i.e., $F^\mu = 1$). In the ABC_2 chalcopyrites the BC

bond contributes most to the nonlinearity and as $F^{\mu}=\frac{1}{2}$, these crystals are therefore not as good as a hypothetical tetrahedral crystal composed entirely of BC bonds would be.

The other factor in Eq. (47), and the most interesting physically, is the individual bond nonlinearity β. As mentioned previously, the large G_{ijk} and N_b of the chalcopyrites, as well as their phase-matching characteristics, make them very favorable nonlinear materials. Since these $A^{II}B^{IV}C_2^V$'s have a disadvantage in bond density (i.e., $F^{\mu}=\frac{1}{2}$) with respect to the $A^{III}B^V$ zinc-blende crystals ($F^{\mu}=1$), one might guess that they would have smaller d_{36} coefficients than their zinc-blende analogs. This, however, is not the case. To see this we first digress slightly and note that Eq. (51) shows that β increases rapidly with decreasing E_g ($\beta \propto E_g^{-6}$ when the dependence of χ on the gap is included) and therefore experimentally one wants to use materials with the smallest possible average gap consistent with transparency in the wavelength region of interest. Since the gap which determines the transparency range is the minimum gap $E_{\min}$ (not the average gap E_g), it is advantageous for a crystal to have a direct gap. This is true because for the same E_g and hence β (other things being equal) an indirect material will have a reduced transparency range. We see, therefore, that when comparing the relative nonlinear coefficients of various materials for a particular wavelength range, it makes sense to compare crystals with similar values for $E_{\min}$.

We now return to our discussion of the relative nonlinearities in zinc-blende and chalcopyrite compounds, and compare GaAs ($E_{\min}=1.44$ eV)[74] with $CdGeP_2$ ($E_{\min}=1.72$ eV).[75] In spite of the fact that GaAs has a significantly smaller $E_{\min}$, and a greater bond density ($F^{\mu}=1$), $CdGeP_2$ has a somewhat larger nonlinear coefficient $d_{36}(CdGeP_2)=260\times10^{-9}$ esu[76] while $d_{36}(GaAs)=215\times10^{-9}$ esu.[77] This larger nonlinearity shows up even more clearly in the Miller's Δ's since $\Delta_{36}(CdGeP_2)=0.71\times10^{-6}$ esu,[76] which is significantly larger than the value $\Delta_{36}(GaAs)=0.46\times10^{-6}$ esu.[77] Thus, the $A^{II}B^{IV}C_2^V$ chalcopyrites can actually have *larger* nonlinearities than their corresponding $A^{III}B^V$ analogs. This is particularly important in view of their phase-matching characteristics. The reason for this result is that the ionicity $f_i=0.23$ of the Ge-P bond[1] [which contributes most to $d_{36}(CdGeP_2)$] is significantly closer to the optimum value $f_i=\frac{1}{6}$ in Fig. 3 than is $f_i(GaP)=0.32$.[1] In view of the favorable nonlinear properties of these $A^{II}B^{IV}C_2^V$ chalcopyrites it will be difficult to find materials with larger nonlinearities in the infrared spectral region. For example, even the unusual, highly anisotropic crystal Se (which has a minimum gap which is similar to GaAs or $CdGeP_2$) has a nonlinear coefficient $d_{11}=230\times10^{-9}$ esu[78] which is slightly smaller than $d_{36}(CdGeP_2)$.

We now turn to a consideration of the visible spectral region, where the $A^{II}B^{IV}C_2^V$ compounds are no longer useful since they are too covalent and thus their band gaps are too small. The oxides form one of the largest and best known classes of visibly transparent materials, and we begin with them. It should be noted that some covalent oxides can have a very serious drawback which may severely reduce their usefulness. This is because the covalent radius of the O atom is rather small and the size term $\Delta(E_h)$ can be comparable to the electronegativity term $\Delta(C)$. This leads to a near cancellation and a small nonlinearity, e.g., BeO, $LiGaO_2$, or $NaBrO_3$. Further, since even a partial cancellation between these contributions reduces the over-all nonlinearity, e.g., ZnO, SiO_2, GeO_2, $NaClO_3$, $AlPO_4$, and $GaPO_4$, generally speaking such materials are unlikely to have the maximum possible nonlinearity. Such cancellations can be avoided, however, in quite ionic oxides, e.g., $f_i\sim0.8$–0.9 since then the O atom has a radius of $r_0\simeq1$ Å and thus the size term can be negligible as in the Nb-O bond in $LiNbO_3$ or $Ba_2NaNb_5O_{15}$. This is one reason for the relatively large β in these materials. Since these niobates have strong d-electron contributions to β, we now consider the general question of whether such d electrons are advantageous or not.

The usefulness of the d electrons depends on a number of factors. Consider for example CuCl. Owing to the strong exciton absorption[51] connected with the d electrons, the useful minimum gap is reduced to $E_{\min}\approx3.2$ eV, which is significantly below ZnS ($E_{\min}=3.8$ eV).[79] In addition, there is a partial cancellation in CuCl between the positive size term ($r_{Cl}>r_{Cu}$) and the negative electronegativity term produced by the d electrons, reducing the net nonlinearity by over a factor of 2. (This cancellation is even more severe in CuBr and CuI). The result is that even with the lower $E_{\min}$ in CuCl, $d_{36}(CuCl)=15\times10^{-9}$ esu[80,81] is significantly smaller than $d_{36}(ZnS)=39\times10^{-9}$ esu.[77]

It is interesting to note that in spite of this lower d_{36} coefficient, CuCl has about the same Δ_{36} as ZnS. This is due to the general increase of Δ with f_i [$f_i(CuCl)>f_i(ZnS)$] which offsets the partial cancellation in CuCl. Another type of cancellation in d-electron compounds occurs between bonds having opposite signs for β, as exemplified by the $A^IB^{III}C_2^{VI}$ system. For $CuInS_2$ this cancellation is particularly severe. None of these deleterious effects is significant in say $LiNbO_3$ or $Ba_2NaNb_5O_{15}$ since $\rho\approx0$, and further, the Nb-O bond β is by far the most significant contributor to the total nonlinearity.

Owing to their large indices of refraction the

sulfides are especially good candidates for large nonlinear coefficients in the visible. In the infrared we just discussed the reasons why the $A^{II}B^{IV}C_2^{V}$ chalcopyrites are found[76] to be excellent nonlinear materials and for somewhat similar reasons the more-ionic larger-band-gap $A^{I}B^{III}C_2^{VI}$ sulfide crystals[82,83] are also superior nonlinear compounds. However, as previously remarked, the noble metals are not ideal for the A atoms; the alkali metals would be better. For example, in spite of the partial cancellation in $AgGaS_2$ which reduces d_{36} by ≈ 2, its other favorable properties (e.g., large G_{36} and N_b) compensate sufficiently, so that its net nonlinear susceptiblity is comparable to that of $Ba_2NaNb_5O_{15}$ in the visible.[83] Thus, if an alkali metal could be used, e.g., $LiGaS_2$, and if the structure *remained the same* (i.e., chalcopyrite) then one would expect a nonlinear coefficient significantly larger than that of $Ba_2NaNb_5O_{15}$. However, there are indications[84] that $LiGaS_2$ is a wurtzitelike structure (similar to $LiGaO_2$). Since, as previously noted, the phase matchable geometrical factor for wurtzite is $\sqrt{3}$ times smaller than that for the chalcopyrites, the net useful nonlinear coefficient of $LiGaS_2$ will probably be comparable to $Ba_2NaNb_5O_{15}$.

The interesting new crystal $InPS_4$ has recently been measured[85] to have a nonlinear susceptibility significantly larger than $Ba_2NaNb_5O_{15}$, but unfortunately it is not phase matchable for harmonic generation in the visible. When its structure becomes known it will be interesting to investigate

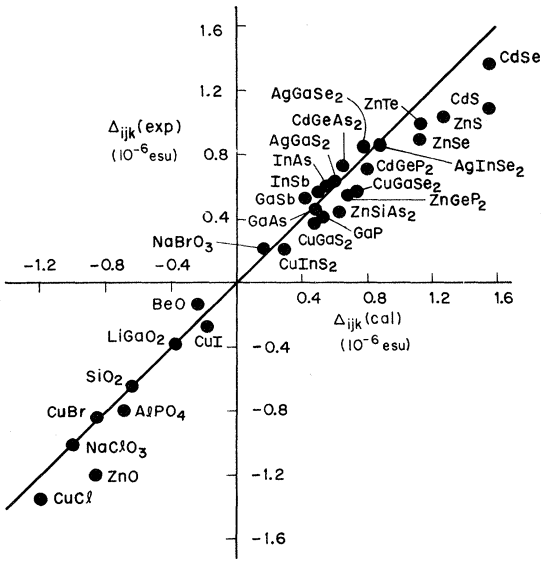

FIG. 5. Plot of experimental-vs-theoretical Miller's Δ's for most of the compounds considered in this paper for which data are available. The agreement between theory and experiment is excellent as demonstrated by small standard deviation of only 18%.

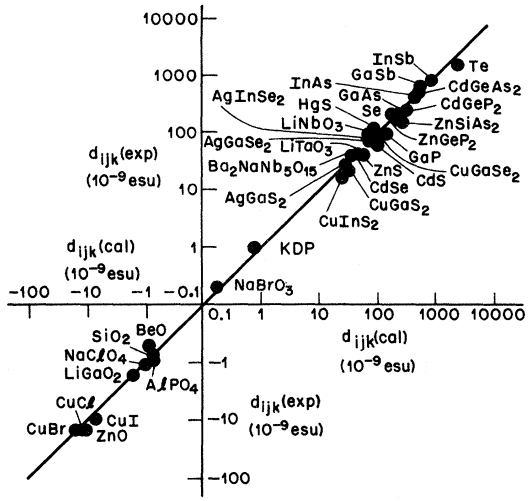

FIG. 6. Plot of experimental-vs-theoretical nonlinear optical susceptibilities for all of the compounds considered in this paper for which data are available (for the polar crystals d_{33} is plotted). The origin for the positive quadrant is $+0.1\times10^{-9}$ esu, while that for the negative quadrant is -0.1×10^{-9} esu. The agreement between theory and experiment is excellent as demonstrated by the small standard deviation of only 19%. This agreement extends over a factor of ~ 4000 in the magnitude of d_{ijk}^{expt}.

it theoretically. Some new compounds (not yet measured) which are likely candidates for visible nonlinearities larger than $Ba_2NaNb_5O_{15}$ are the defect chalcopyrites such as $ZnGa_2S_4$ and $CdGa_2S_4$.

XVIII. SUMMARY

Some of our theoretical results are summarized in Figs. 5 and 6, where Δ_{ijk}(expt) or d_{ijk}(expt) is plotted against Δ_{ijk}(calc) or d_{ijk}(calc). Figure 5 includes most of the compounds for which experimental data are available (except for the materials in Tables XV and XVI) while Fig. 6 includes *all* the compounds. The excellent agreement between our theory and experiment is evident, being 18 and 19% for Figs. 5 and 6, respectively,[86] and is achieved without the benefit of fitting any parameters to the nonlinear susceptibility. Our simple bond-charge calculation is thus able to accurately account for a wide variety of crystals such as $A^{III}B^{V}$ (e.g., GaP, GaAs, GaSb, InAs, InSb), $A^{II}B^{VI}$ (e.g., ZnS, ZnSe, ZnTe, CdS, CdSe), $A^{I}B^{VII}$ (e.g., CuCl, CuBr, CuI), crystals possessing widely different-sized atoms (e.g., ZnO, BeO, CuI, SiO_2, $LiGaO_2$, $NaClO_3$, $AlPO_4$), crystals having high or low ionicities [e.g., f_i(Te) $= 0.05 f_i$(CuCl) $= 0.88$], large or small gaps [$E_{\min}$(InSb) $= 0.24$ eV, $E_{\min}$(BeO) ~ 10 eV], positive or negative nonlinearities, crystals possessing strong d-electron contributions (e.g., CuCl, CuBr, CuI, $AgGaS_2$, $CuGaS_2$, $AgGaSe_2$, $CuGaSe_2$, $AgInSe_2$, $CuInS_2$, $LiNbO_3$, $Ba_2NaNb_5O_{15}$, $LiTaO_3$), multibond

crystals [e.g., $A^{I}B^{III}C_2^{VI}$ ($LiGaO_2$, $AgGaSe_2$), $A^{II}B^{IV}C_2^{V}$ ($CdGeP_2$, $ZnGeP_2$, $CdGeAs_2$, $ZnSiAs_2$), $A^{III}B^{V}C_2^{VI}$ ($AlPO_4$), and KH_2PO_4], and highly anisotropic crystals (HgS, Se, Te). The magnitude of the nonlinearity varies by a factor of 25 for $|\Delta_{ijk}|$ [$\Delta_{33}^{expt}(BeO) = -0.13\times10^{-6}$ esu, $\Delta_{33}^{expt}(LiNbO_3) = +3.3\times10^{-6}$ esu], while the variation in $|d_{ijk}|$ is a factor of ~4000 [$d_{14}^{expt}(NaBrO_3) = +0.43\times10^{-9}$ esu, $d_{11}^{expt}(Te) = 1550\times10^{-9}$ esu]. We have also treated the difficult problem of determining the functional dependence of β on the bond length, and were thus able to calculate all the tensor components of Δ_{ijk} for such important materials as $LiNbO_3$, $LiTaO_3$, and $Ba_2NaNb_5O_{15}$.

One of the reasons for the success of our bond-charge model is that most of the potentially troublesome local-field effects are automatically included by our use of the macroscopic linear susceptibility. Further, our theory of the nonlinear susceptibility is approximately self-consistent since unknown parameters are determined from the linear susceptibility; e.g., the ionicity is determined dielectrically, and the single proportionality constant in the relation for q is determined from a best fit to the linear susceptibility. Finally, the model includes in a simple way the three important contributions to the nonlinearity, i.e., the bond ionicity, the difference in the atomic radii of the atoms composing the bond, and d-electron contributions.

We have also discussed some of the desirable characteristics that lead to a large nonlinearity, and found that in the infrared the $A^{II}B^{IV}C_2^{V}$ chalcopyrites will be hard to improve upon, whereas in the visible $Ba_2NaNb_5O_{15}$ (which presently has the largest phase-matchable nonlinearity in this spectra region) leaves some room for improvement (we suggested, for example, $CdGa_2S_4$).

Note added in proof. Recently, the nonlinearity of CdTe has been measured by Sherman and Coleman [J. Appl. Phys. 44, 238 (1973)]. Their result $\Delta_{14}(CdTe) = 1.32\times10^{-6}$ esu is in good agreement with our calculated value from Table III, $\Delta_{14}(CdTe) = 1.39\times10^{-6}$ esu. The nonlinearity of AgI has also been recently measured [B. F. Levine, W. A. Nordland, and J. W. Shiever, IEEE J. Quantum Electron. QE-9, April (1973) (to be published)]. The result $\Delta_{33}(AgI) = -1.76\times10^{-6}$ esu is in agreement with the theoretical value in Table VI, namely, $\Delta_{33}(AgI) = (2/\sqrt{3})\,\Delta_{14}(AgI) = -1.35\times10^{-6}$ esu. Also our theory has been used successfully on the *quaternary* compounds Zn_3AgInS_5 and Zn_5AgInS_7 [B. F. Levine, C. G. Bethea, V. G. Lambrecht, Jr., and M. Robbins, IEEE J. Quantum Electron. QE-9, Feb. (1973)]. Finally, we have been able, for the first time, to directly and accurately calculate the higher-order acoustically induced optical harmonic generation coefficient, using exactly the same theory described here [e.g., Eq. (93) in particular]. [B. F. Levine, Phys. Rev. Lett. 30, 171 (1973).]

ACKNOWLEDGMENTS

I am especially indebted to R. C. Miller and W. A. Nordland for making their experimental measurements available prior to publication. Without their crucial measurements (e.g., the magnitude and sign of d_{14} in CuI) our treatment of the noble-metal d electrons would have been incomplete. It is also a pleasure to acknowledge many helpful discussions with R. C. Miller, J. A. Van Vechten, J. A. Giordmaine, D. A. Kleinman, S. H. Wemple, and M. DiDomenico.

APPENDIX

Consider the anharmonic oscillator

$$\ddot{z} + \omega_0^2 z + vz^2 = (eE_z\cos\omega t)/m \ . \tag{A1}$$

It is easily seen that the term in the solution of (A1) that oscillates like $\cos2\omega t$ is (for $\omega \ll \omega_0$)

$$z(2\omega) = -\frac{1}{2}\,\frac{ve^2}{m^2\omega_0^6}\,E_z^2\cos2\omega t \ . \tag{A2}$$

This produces a polarization at 2ω of $P_z(2\omega) = ez(2\omega)$. Since the second-harmonic coefficient β_{zzz} is simply defined by $P_z(2\omega) \equiv \beta_{zzz}E_z^2\cos2\omega t$ we have

$$\beta_{zzz} = -\tfrac{1}{2}\,ve^3/m^2\omega_0^6 \ . \tag{A3}$$

Let us now ask how the resonant frequency of the oscillator (A1) changes when a dc field $\mathcal{E}_z$ is applied. For clarity assume $\mathcal{E}_z \gg E_z$ so that E_z is an infinitesimal oscillating probe field.

The equilibrium position of the oscillator will change from $z = 0$ to $z_0 = e\mathcal{E}_z/m\omega_0^2$ while the frequency of oscillation for an infinitesimal displacement Δz from this new equilibrium position (ω_0') has changed to

$$\begin{aligned} &-(\omega_0')^2\Delta z + \omega_0^2\Delta z + 2vz_0\Delta z = 0 \ , \\ &(\omega_0')^2 = \omega_0^2 + 2vz_0 = \omega_0^2 + 2ve\mathcal{E}_z/m\omega_0^2 \ . \end{aligned} \tag{A4}$$

Using $\chi = e^2/m(\omega_0')^2$ we find that the change in the susceptibility caused by the field $\mathcal{E}$ is given by

$$\Delta\chi_{zzz} = -2ve^3\mathcal{E}_z/m^2\omega_0^6 \ . \tag{A5}$$

Comparing Eqs. (A3) and (A5) we find

$$\beta_{zzz} = \tfrac{1}{4}\,\Delta(\chi_b^{\mu})_{zz}/\mathcal{E}_t \ , \tag{A6}$$

showing that the numerical factor of $\frac{1}{4}$ appearing in Eq. (45) is correct.

---

[1] B. F. Levine (unpublished), hereafter referred to as III.

[2] B. F. Levine, Phys. Rev. B 7, 2591 (1973); hereafter referred to as II.

[3] J. A. Armstrong, N. Bloembergen, J. Ducuing, and P. S.

Pershan, Phys. Rev. **127**, 1918 (1962).
[4]R. Loudon, Proc. R. Soc. Lond. **80**, 952 (1962).
[5]P. L. Kelley, J. Phys. Chem. Solids **24**, 607 (1963); J. Phys. Chem. Solids 24, 1113 (1963).
[6]P. N. Butcher and T. P. McLean, Proc. R. Soc. Lond. **81**, 219 (1963).
[7]N. Bloembergen and Y. R. Shen, Phys. Rev. **133**, A37 (1964).
[8]J. F. Ward and P. A. Franken, Phys. Rev. **133**, A183 (1964).
[9]H. Cheng and P. B. Miller, Phys. Rev. **134**, A683 (1964).
[10]J. A. Giordmaine, Phys. Rev. **138**, A1599 (1965).
[11]I. Freund and B. F. Levine, Phys. Rev. Lett. **23**, 854 (1969).
[12]F. N. H. Robinson, Bell Syst. Tech. J. **46**, 913 (1967), J. Phys. C **1**, 286 (1968).
[13]S. S. Jha and N. Bloembergen, Phys. Rev. **171**, 891 (1968).
[14]Chr. Flytzanis and J. Ducuing, Phys. Rev. **178**, 1218 (1969); J. Ducuing and Chr. Flytzanis, in *Optical Properties of Solids*, edited by F. Abelès (North-Holland, Amsterdam, 1971).
[15]N. Bloembergen, R. K. Chang, and J. Ducuing, in *Physics of Quantum Electronics*, edited by P. L. Kelley, B. Lax, and P. E. Tannenwald (McGraw–Hill, New York, 1966), p. 67.
[16]D. E. Aspnes, Phys. Rev. B **6**, 4648 (1972).
[17]M. I. Bell, in *Electronic Density of States*, edited by L. H. Bennett, Natl. Bur. Std. (U. S.) Spec. Publ. No. 323 (U.S. GPO, Washington, D.C., 1971) p. 757; Phys. Rev. B **6**, 516 (1972).
[18]R. C. Miller, Appl. Phys. Lett. **5**, 17 (1964).
[19]See, for example, J. A. Giordmaine, in *Quantum Electronics III*, edited by P. Grivet and N. Bloembergen (Columbia U. P., New York, 1964), Vol. II, p. 1549; N. Bloembergen, *Nonlinear Optics* (Benjamin, New York, 1965).
[20]C. G. B. Garrett and F. N. H. Robinson, IEEE J. Quantum Electron. **2**, 328 (1966).
[21]C. G. B. Garrett, IEEE J. Quantum Electron. **4**, 70 (1968).
[22]S. K. Kurtz and F. N. H. Robinson, Appl. Phys. Lett. **10**, 62 (1967).
[23]R. A. Soref, IEEE J. Quantum Electron. **5**, 126 (1969).
[24]C. R. Jeggo, J. Phys. C **5**, 330 (1972).
[25]F. N. H. Robinson, Phys. Lett. A **26**, 435 (1968).
[26]C. R. Jeggo, Phys. Lett. A **29**, 177 (1969).
[27]C. R. Jeggo and G. D. Boyd, J. Appl. Phys. **41**, 2741 (1970); C. R. Jeggo, Opt. Commun. **1**, 375 (1970).
[28]M. DiDomenico, Jr. and S. H. Wemple, J. Appl. Phys. **40**, 720 (1969).
[29]C. L. Tang and Chr. Flytzanis, Phys. Rev. B **4**, 2520 (1971).
[30]J. Jerphagnon, Phys. Rev. B **1**, 1739 (1970).
[31]J. C. Phillips and J. A. Van Vechten, Phys. Rev. **183**, 709 (1969).
[32]D. A. Kleinman, Phys. Rev. B **2**, 3139 (1970).
[33]B. F. Levine, Phys. Rev. Lett. **22**, 787 (1969); Phys. Rev. Lett. **25**, 440 (1970).
[34]R. C. Miller, W. A. Nordland, S. C. Abrahams, J. L. Bernstein, and C. Schwab, Phys. Rev. (to be published). B. F. Levine, C. G. Bethea, V. G. Lambrecht, Jr., and M. Robbins, IEEE J. Quantum Electron QE-9, Feb. 1973. B. F. Levine, W. A. Nordland, and J. W. Shiever, IEEE J. Quantum Electron QE-9, Apr. 1973 (to be published).
[35]D. S. Chemla, Phys. Rev. Lett. **26**, 1441 (1971).
[36]For several recent reviews of these areas, see *The Laser Handbook*, edited by F. T. Arecchi and E. O. Schultz-Du Bois (North-Holland, Amsterdam, 1972). For additional references see Ref. 66.
[37]J. C. Phillips, Phys. Rev. Lett. **20**, 550 (1968).
[38]J. A. Van Vechten, Phys. Rev. **182**, 891 (1969); Phys. Rev. **187**, 1007 (1969).
[39]See, for example, J. C. Phillips, Phys. Rev. **166**, 832 (1968); Phys. Rev. **168**, 905 (1968); Phys. Rev. **168**, 911 (1968); Phys. Rev. **168**, 917 (1968); R. M. Martin, Phys. Rev. **186**, 871 (1969); J. P. Walter and M. L. Cohen, Phys. Rev. B **4**, 1877 (1971).
[40]See, for example, B. Dawson, Proc. R. Soc. Lond. **298**, 264 (1967); **298**, 379 (1967); **298**, 395 (1967); R. Uno, T. Okano, and K. Yukino, J. Phys. Soc. Jap. **28**, 437 (1970).
[41]J. C. Phillips, Phys. Rev. **166**, 832 (1968).
[42]See, for example, Ref. 14.
[43]J. A. Van Vechten and J. C. Phillips, Phys. Rev. B **2**, 2160 (1970).
[44]For a discussion of the conversion of esu units (i.e., cm/statvolts) to mks units see, for example, R. Beckman and S. K. Kurtz, in Landolt-Börnstein, *Numerical Data and Functional Relationships*, edited by K. H. Hellwege and A. M. Hellwege (Springer, Berlin, 1969), New Series Group III, Vol. 2; or S. Singh, *Handbook of Lasers* (Chemical Rubber Co., Cleveland, 1971).
[45]I. P. Kaminow and W. D. Johnson, Jr., Phys. Rev. **160**, 519 (1967); see also Appendix 2 in G. D. Boyd and D. A. Kleinman, J. Appl. Phys. **39**, 3597 (1968); and S. H. Wemple and M. Di Domenico, Jr., in *Applied Solid State Science*, edited by R. Wolfe (Academic, New York, 1972), Vol. 3.
[46]In fact, Flytzanis and Ducuing (Ref. 14) (see Ref. 29), Levine (Ref. 33), and Tang and Flytzanis (Ref. 29) have all made such errors of a factor of 2.
[47]D. A. Kleinman, Phys. Rev. **126**, 1977 (1962).
[48]L. Pauling, *The Nature of the Chemical Bond* (Cornell U. P., Ithaca, 1960); J. C. Slater, *Quantum Theory of Molecules and Solids* (McGraw–Hill, New York, 1965), Vol. 2; F. Zachariasen (unpublished), quoted by C. Kittel, *Introduction to Solid State Physics* (Wiley, New York, 1966); R. D. Shannon and C. T. Prewitt, Acta Crystallogr. B **25**, 925 (1969).
[49]See, for example, F. G. Parsons and R. K. Chang, Opt. Commun. **3**, 173 (1971).
[50]In order to average out any slight inaccuracies in the calculation we have simply used (see Ref. 1) $b=1.62$ for all the $A^{III}B^{V}$ and $A^{II}B^{VI}$ zinc-blende and wurtzite crystals.
[51]M. Cardona, Phys. Rev. **129**, 69 (1963).
[52]K. S. Song, J. Phys. Radium 28, 195 (1967); J. Phys. Chem. Solids **28**, 2003 (1967).
[53]J. B. Anthony, A. D. Brothers, and D. W. Lynch, Phys. Rev. B **5**, 3189 (1972).
[54]S. Kono, T. Ishii, T. Sagawa, and T. Kobayasi, Phys. Rev. Lett. **28**, 1385 (1972).
[55]J. C. Slater, Phys. Rev. **36**, 57 (1930).
[56]L. Pauling, *The Nature of the Chemical Bond* (Cornell U. P., Ithaca, 1960).
[57]S. Singh, J. R. Potopowicz, J. G. Van Uitert, and S. H. Wemple, Appl. Phys. Lett. **19**, 53 (1971).
[58]BeO and CuI are not included in this average σ, owing to the very close cancellations involved. A true measure of the agreement between theory and experiment for these compounds is $\sim 10\%$, since, as discussed in the text, a variation of $\Delta(C)$ or $\Delta(E_h)$ by this amount will give a coincidence between the two.
[59]R. W. G. Wyckoff, *Crystal Structures* (Interscience, New York, 1948).
[60]H. J. Simon and N. Bloembergen, Phys. Rev. **171**, 1104 (1968).
[61]M. Marezio, Acta Crystallogr. **18**, 481 (1965).
[62]J. L. Shay. B. Tell, H. M. Kasper, and L. M. Schiavone, Phys. Rev. B **5**, 5003 (1972); B. Tell, J. L. Shay, and H. M. Kasper, Phys. Rev. B **6**, 3008 (1972).
[63]See, for example, F. Jona and G. Shirane, in *Ferroelectric Crystals*, edited by R. Smoluchowski and N. Kurti (Pergamon, New York, 1962).
[64]J. P. van der Ziel and N. Bloembergen, Phys. Rev. **135**, A1662 (1964).

[65]W. A. Nordland, Ferroelectrics 2, 57 (1971); B. F. Levine and C. G. Bethea, Appl. Phys. Lett. 20, 272 (1972).

[66]See, for example, G. D. Boyd, R. C. Miller, K. Nassau, W. L. Bond, and A. Savage, Appl. Phys. Lett. 5, 234 (1964); R. L. Byer, S. E. Harris, D. J. Kuizenga, J. F. Young, and R. S. Feigelson, J. Appl. Phys. 40, 444 (1969); R. L. Byer and S. E. Harris, Phys. Rev. 168, 1064 (1968); S. Singh, D. A. Draegert, and J. E. Geusic, Phys. Rev. B 2, 2709 (1970); F. R. Nash, E. H. Turner, P. M. Bridenbaugh, and J. M. Dziedzic, J. Appl. Phys. 43, 1 (1972); R. C. Miller, W. A. Nordlund, and P. M. Bridenbaugh, J. Appl. Phys. 42, 4145 (1971); See, for example, J. A. Giordmaine and R. C. Miller, Phys. Rev. Lett. 14, 973 (1965); R. C. Miller and W. A. Nordland, Appl. Phys. Lett. 10, 53 (1967); S. E. Harris, Proc. IEEE 57, 2096 (1969); E. O. Ammann, J. M. Yarborough, M. K. Oshman, and P. C. Montgomery, Appl. Phys. Lett. 16, 309 (1970); R. G. Smith, in *Laser Handbook*, edited by F. T. Arecchi and E. O. Shultz-Du Bois (North-Holland, Amsterdam, 1972); L. B. Kreuzer, Appl. Phys. Lett. 10, 336 (1967); Appl. Phys. Lett. 13, 57 (1968).

[67]See, for example, S. Singh's chapter in *Handbook of Lasers* (Chemical Rubber Co., Cleveland, 1971).

[68]S. C. Abrahams, J. M. Reddy, and J. L. Bernstein, J. Phys. Chem. Solids 27, 997 (1966); P. B. Jamieson, S. C. Abrahams, and J. L. Bernstein, J. Chem. Phys. 50, 4352 (1969); S. C. Abrahams, W. C. Hamilton, and A. Sequeira, J. Phys. Chem. Solids 28, 1693 (1967).

[69]R. C. Miller, W. A. Nordland, and P. M. Bridenbaugh, J. Appl. Phys. 42, 4145 (1971).

[70]S. C. Abrahams, S. K. Kurtz, and P. B. Jamieson, Phys. Rev. 172, 551 (1968).

[71]R. C. Miller, W. A. Nordland, and A. A. Ballman, Opt. Commun. 6, 210 (1972); S. Singh, J. P. Remeika, and J. R. Potopowicz, Appl. Phys. Lett. 20, 135 (1972).

[72]$PbTiO_3$ is a particularly interesting example and we leave the treatment of it and the isomorphic compound $BaTiO_3$ for a later publication.

[73]From Eq. (56), $G_{ijk} = \Delta_{ijk} / N_b \Delta_\beta$.

[74]M. D. Sturge, Phys. Rev. 127, 768 (1962).

[75]J. L. Shay, E. Buehler, and J. H. Wernick, Phys. Rev. B 4, 2479 (1971).

[76]G. D. Boyd, E. Buehler, F. G. Storz, and J. H. Wernick, IEEE J. Quantum Electron. 8, 419 (1972); R. L. Byer, H. Kildal, and R. S. Feigelson, Appl. Phys. Lett. 19, 237 (1971).

[77]B. F. Levine and C. G. Bethea, Appl. Phys. Lett. 20, 272 (1972).

[78]G. W. Day, Appl. Phys. Lett. 18, 347 (1971).

[79]M. Cardona, Solid State Phys. Suppl. 11 (1969).

[80]D. Chemla, P. Kupecek, C. Schwartz, C. Schwab, and A. Goltzene, IEEE J. Quantum Electron. 7, 126 (1971).

[81]R. C. Miller, W. A. Nordland, S. C. Abrahams, and C. Schwab Phys. Rev. B (to be published).

[82]G. D. Boyd, H. Kasper, and J. H. McFee, IEEE J. Quantum Electron. 7, 563 (1971); G. D. Boyd, H. M. Kasper, J. H. McFee, and F. G. Storz, IEEE J. Quantum Electron. QE-8, 900 (1972).

[83]J. P. van der Ziel and W. A. Nordland (unpublished), quoted in G. D. Boyd, H. Kasper, and J. H. McFee, IEEE J. Quantum Electron. 7, 563 (1971).

[84]H. Kasper (private communication).

[85]P. M. Bridenbaugh (unpublished).

[86]The compounds which have close cancellations between the ionic and radii contributions (BeO, CuI, $NaBrO_3$, $LiGaO_2$, and $CuInS_2$) are not included in these standard deviations σ. However, as noted previously, the *actual* discrepancy between theory and experiment for these crystals is well within the 18–19% overall deviation. The highly anisotropic crystals in Table XVI are also not included in evaluating σ. However, even if the exceptions noted above are included, the deviation for *all* the crystals considered is still only 24%.

PHYSICAL REVIEW B VOLUME 7, NUMBER 6 15 MARCH 1973

Scattering of Phonons by Bound and Free Electrons in Sb-Doped Ge in the Temperature Range 6–80 °K

M. Singh and G. S. Verma

Physics Department, Banaras Hindu University, Varanasi-5, India

(Received 1 June 1972)

It has been established in the present work that the expressions obtained by Kumar, Srivastava, and Verma for the relaxation rates due to the resonance scattering of phonons by bound donor electrons can account very well for the phonon-conductivity results of Sb-doped Ge for donor-electron concentrations less than 10^{17} cm^{-3}. Elastic scattering alone can account for the drastic reduction in the phonon conductivity with doping. For donor-electron concentrations greater than 5×10^{17} cm^{-3}, the observed drastic reduction in the phonon conductivity can be accounted for by the scattering of phonons by electrons in the conduction state. This is possible because of the merger of the impurity states with the conduction states for such heavily doped materials. The density-of-states effective mass is found to vary from $0.56m_0$ to $0.82m_0$ in the temperature range 6–80 °K.

I. INTRODUCTION

Extensive measurements of thermal conductivity of n-type Ge in the low-temperature range have been carried out by Pearlman's group[1–5] at Purdue University. The experimental results are usually depicted as phonon-conductivity–versus–temperature curves, which show a maximum at about (10–15) °K. At temperatures below the conductivity maximum, electron-phonon scattering plays a very important part in determining the resistivity of the material. For high concentrations of dopant, phonons are scattered by donor electrons in the conduction state, and for low concentrations by bound donor electrons. The theory of the scattering of phonons by bound donors has been considered by